

# We are IntechOpen, the world's leading publisher of Open Access books Built by scientists, for scientists

6,900

Open access books available

186,000

International authors and editors

200M

Downloads

Our authors are among the

154

Countries delivered to

TOP 1%

most cited scientists

12.2%

Contributors from top 500 universities



WEB OF SCIENCE™

Selection of our books indexed in the Book Citation Index  
in Web of Science™ Core Collection (BKCI)

Interested in publishing with us?  
Contact [book.department@intechopen.com](mailto:book.department@intechopen.com)

Numbers displayed above are based on latest data collected.  
For more information visit [www.intechopen.com](http://www.intechopen.com)



# Polycation-Mediated Gene Delivery: The Physicochemical Aspects Governing the Process

Manuel Alatorre-Meda<sup>1</sup>, Eustolia Rodríguez-Velázquez<sup>2</sup>  
and Julio R. Rodríguez<sup>3</sup>

<sup>1</sup>*Grupo de Física de Coloides y Polímeros, Departamento de Física de la Materia Condensada. Facultad de Física, Universidad de Santiago de Compostela*

<sup>2</sup>*Master student. Master en Ciencia y Tecnología de Materiales, Facultad de Física Universidad de Santiago de Compostela*

<sup>3</sup>*Grupo de Nanomateriales y Materia Blanda, Departamento de Física de la Materia Condensada. Facultad de Física, Universidad de Santiago de Compostela Spain*

## 1. Introduction

### 1.1 Chapter objectives

Gene therapy is the process by which a foreign, corrective (or missing) gene is inserted toward biological tissues or cells aiming to alleviate symptoms or prevent disorders. Several clinical trials have demonstrated gene therapy as a promising option to treat diseases. However, therapeutic biological limitations (such as adverse immune responses of the body to incoming gene delivery systems) coupled with a poor understanding of the physicochemical motifs involved in the DNA compaction and delivery (transfection) processes have resulted in non-100% effective protocols. Aiming to contribute to a better understanding of the different physicochemical aspects of gene therapy, our group has committed for some years now to the physical chemistry characterization of the DNA compaction and transfection mediated by different kinds of compacting agents (vectors).

In this chapter, we present an overview of the results we have obtained during the last three years regarding the DNA compaction and transfection mediated by cationic-liposomes and -polymers (polycations). Two families of polycations, Chitosan and Poly (diallyldimethylammonium chloride) (pDADMAC), and one cationic lipid formulation extensively used worldwide in transfection assays, Metafectene® Pro (MEP), are studied as DNA vectors and compared with other systems already published. In particular, by varying the solution pH and polycation characteristics (chemical composition and molecular weight), we assess the influence of polycation-charge density (i.e., the mole fraction of the ionized groups along the polymer chain) and -valence (i.e., the total charge per polymer chain) on different parameters of the complexes formed that are important for gene therapy. The studied parameters include i) the hydrodynamic radius,  $R_H$ , ii) the stability with time, iii) the vector to DNA ratio at which complexation takes place iv) the  $\zeta$ -potential, v) the

binding energetics, vi) the morphology, and vii) the transfection efficiency. The physicochemical characterization was carried out by means of different experimental techniques including dynamic and static light scattering (DLS and SLS), electrophoretic mobility, isothermal titration calorimetry (ITC), transmission electron- and atomic force microscopy (TEM and AFM), and conductometry at 25 °C. Transfection experiments were conducted at standard culture conditions and evaluated by means of the  $\beta$ -galactosidase ( $\beta$ -gal) and luciferase assays at 25 °C. Outstanding results concerning the electrochemical and energetic features of the complexes with higher transfection efficiencies are fully discussed.

## 1.2 Gene therapy

The possibility to treat diseases by the insertion of genes into human cells and tissues has proposed gene therapy as the therapy of the 21st century (Verma & Somia, 1997). With the first clinical trial reported in the early 1990s (Anderson, 1990), protocols for several, diverse disorders have been conducted and promising results have been obtained (O'Connor & Crystal, 2006); however, a single protocol suitable to be applied as a routinely means to treat any particular disease is far to be achieved.

In practice, the entrance of naked, exogenous DNA to the cell nucleus results problematic due to different extra and intracellular barriers. On the one hand, systemic circulation of DNA is hindered by nuclease degradation (Nguyen et al., 2009). On the other hand, the electrolytic nature of DNA gives rise to electrostatic repulsions as DNA approaches to cells provided that both DNA and cell membranes are negatively charged (due to the phosphate groups distributed by the outside of the polymer helices and the several proteoglycans constituting the cell membranes) (Tros de Ilarduya et al., 2010). Also, once inside cells, steric restrictions are expected to hamper the DNA transportation to the cell nucleus given that mobility of free DNA based on diffusion in the cytoplasm is negligible (Dowty et al., 1995), possibly due to cytoskeletal elements within the cytoplasm that function as molecular sieves and prevent the diffusion of large molecules (Lubyphelps et al., 1987). Thus, for exogenous DNA to be properly transferred to living cells (and tissues), all these extra and intracellular barriers must be circumvented.

Current gene transfer protocols rely on the use of natural and synthetic DNA complexing agents, referred to as vectors or gene carriers, to compact, protect, and provoke a charge inversion of DNA, surpassing, by this way, the previously cited biological barriers. Vectors are either viral or non-viral. Viral delivery, also known as transduction, involves the packaging of DNA (or in some cases RNA) into a virus particle (Mancheño-Corvo & Martín-Duque, 2006). This procedure is, by far, the most effective one considering the high transfection efficiencies it renders; however, fundamental problems associated with viral vectors, including toxicity and immunogenicity, among others, have encouraged the investigation of safer gene delivery alternatives such as non-viral vectors (Verma & Somia, 1997).

Compared to viruses, non-viral transfection vectors possess many important advantages such as safety, versatility, ease of preparation, and, in some cases, the possibility to transfect DNA fragments of unlimited sizes (Orth et al., 2008). The first approaches using non-viral vectors as gene carriers come from the late 1980s when Felgner and coworkers started to try with cationic liposomes (Felgner et al., 1987). Cationic liposome-DNA complexes, also referred to as lipoplexes, form spontaneously after electrostatic interactions between the positively charged liposomes and the negatively charged DNA, producing physically stable formulations suitable to transfect relatively high amounts of plasmid DNA to cells in culture

(Felgner et al., 1987). Other non-viral vectors subsequently studied include surfactants, proteins (particularly histones), multivalent ions, nanoparticles, and polycations, all of which (also) form electrostatically driven DNA complexes (Gonzalez-Perez & Dias, 2009). In the following sections we explore representative gene delivery systems employing polycations and cationic liposomes as gene carriers.

### 1.3 Cationic-liposomes and -polymers for gene therapy

Polycations and cationic liposomes are the non-viral vectors most commonly studied for gene therapy due to the outstanding characteristics they present. In addition to the potential safety benefits, they offer, for instance, a great structural and chemical versatility for manipulating their physicochemical properties, vector stability upon storage and reconstitution, and a larger gene capacity to transfer DNA as compared to their viral and non-viral counterparts (Dias et al., 2002; Midoux et al., 2009; Tros de Ilarduya et al., 2010). As mentioned before, cationic liposomes were the first class of non-viral vectors showing satisfactory transfection efficiencies. In the first work reporting on lipofection (the lipid-mediated DNA transfection process), Felgner and coworkers employed N-[1-(2,3-dioleoyloxy)propyl]-N,N,N-trimethylammonium chloride (DOTMA), a synthetic cationic lipid, to transfect plasmid DNA to different cells lines in culture (Felgner et al., 1987). Major advantages of utilizing DOTMA containing liposomes were that DNA entrapment inside the lipoplexes was found to be of a 100%. Also, as suggested by fluorescence microscopy data, DOTMA demonstrated to facilitate fusion of the complexes with the plasma membrane of the studied culture cells, resulting in DNA transfer rates from 5- to >100-fold more effective (depending on the transfected cell line) than previous procedures such as the calcium phosphate or the DEAE-dextran transfection techniques (Kucherlapati & Skoultchi, 1984). However, a major drawback was that these liposomes were found to be cytotoxic (Felgner et al., 1987). Following the trail of this pioneering work, other cationic lipids and surfactants have also been tested over the years (Simberg et al., 2004). Unfortunately, the general perspective is that excessive positive charges, facilitating the electrostatic interactions with negatively charged DNA, also promote cytotoxicity. As a result, zwitterionic lipids such as dioleoylphosphatidylethanolamine (DOPE) and cholesterol are nowadays commonly implemented (Tros de Ilarduya et al., 2010).

Polycations (i.e., positively charged polyelectrolytes) are macromolecules attractive to gene therapy for various reasons. Firstly, provided the high charge density they bear, they are considered as the most efficient nucleic acid-condensing agents. Different to other kinds of non-viral vectors like trivalent ions and cationic surfactants, interacting with a few consecutive DNA monomers (bases) (Sarraguca & Pais, 2006), polycations interact with DNA bases that are significantly far apart, promoting bridging between different sites in the DNA chain or between different DNA chains (Dias et al., 2003).

Secondly, because of the strong DNA-polycation interactions, DNA-polycation complexes (polyplexes) are specially effective in what DNA charge masking and extracellular protection concerns (De Smedt et al., 2000). And thirdly, given that they can be functionalized, copolymerized or structurally modified, polycation constructs can be tailored to improve cell-specific therapeutic efficacy with reduced side effects (Ke & Young, 2010). Polycations most frequently studied as gene carriers include poly(L-lysine) (PLL) (G. Y. Wu & C. H. Wu, 1987), polyethylenimine (PEI) (Boussif et al., 1995), chitosan (Mumper et al., 1995), poly( $\beta$ -amino ester)s (Lynn & Langer, 2000), and poly(amido amine) (PAMAM) dendrimers (Haensler & Szoka, 1993). Generally speaking, the basicity

and degree of protonation of polycationic vectors depend on their amount of primary, secondary, and tertiary amines, which greatly influences the cell toxicity, the escape of polyplexes from endosomes, and the transfection efficiency (Behr 1997).

#### **1.4 Physicochemical aspects of relevance for gene therapy**

Gene transfer to eukaryotic cells is a long process encompassing several successive steps. Plasmid DNA must be packaged into complexes/particles first. Next, the DNA-containing complexes/particles must associate with cells and become internalized into them by cellular uptake processes. Following uptake, DNA-containing complexes/particles must escape the endosomal compartment into the cytoplasm and release their DNA-cargo. Finally, DNA must translocate into the cell nucleus to be transcribed into mRNA and subsequently translated into protein antigen (Nguyen et al., 2009). For all these steps to successfully occur, the final characteristics of the lipo- and polyplexes to be employed must, undoubtedly, be studied and tailored. Of especial importance for complex formation and gene delivery, we can enumerate the following physicochemical aspects.

##### **1.4.1 Size and surface charge**

The ability of cationic vectors to condense DNA into nano-sized complexes is believed to be crucial for gene therapy (Sahay et al., 2010; Tros de Ilarduya et al., 2010). DNA compaction, also known as condensation, is a reversible coil to globule transition favored by the binding of cationic vectors to the negatively charged DNA phosphate groups (Bloomfield, 1997). When the number of neutralized charges reaches a critical value, DNA undergoes localized bending or distortion, which facilitates the formation of complexes with sizes much smaller (in the range of nanometers) than that of the DNA coil conformation (in the range of microns) (De Smedt et al., 2000; Wilson & Bloomfield, 1979). Analyzing the impact of experimental conditions on the resulting complex dimensions, several studies have demonstrated that parameters like type, size and modification of the cationic vector, the carrier/DNA charge ratio, and also the protocol of complex formation, can all exert a strong influence (Ogris et al., 1998). On the other hand, with respect to the role of complex size on the cellular internalization mechanism, it has been demonstrated that lipo- and polyplexes with sizes up to 200 nm are taken up by the clathrin-dependent pathway, whereas aggregates larger than 500 nm are internalized via clathrin-independent mechanisms (Rejman et al., 2004; Sahay et al., 2010).

Apart from a reduction in size, binding of cationic vectors to DNA also imparts a positive charge. Although this positive charge is important for both cellular-binding and -internalization, it might also be a cause for concern for in vivo applications since cationic complexes readily bind with serum proteins such as serum albumin, promoting aggregation and blood clearance (Tros de Ilarduya et al., 2010). Additionally, an excess of positive charge, commonly reflected by complexes formed at high vector to DNA ratios, might lead to cytotoxicity provided that negatively charged cell membranes are prone to be damaged in the presence of cationic, extracellular compounds (Thomas & Klibanov, 2003). Thus, a successful gene delivery procedure, pursuing a high transfection efficiency at the lowest possible cytotoxicity, should find a delicate balance in the complex surface charge, that is, the complex must possess a high enough positive charge so as to ensure a proper cell-complex association, but at the same time this necessary positive charge must not cause a lethal damage to the cell.



### 1.4.2 Structural organization

The DNA ordering inside lipoplexes has been reported in the form of four main conformations: one with a short-range lamellar structure composed of flat lipid bilayers and DNA packed between them (Battersby et al., 1998; Dias et al., 2002; Lasic et al., 1997; Radler et al., 1997; Salditt et al., 1997), another where the DNA molecules are encapsulated inside a lipid bilayer forming cylindrical complexes that are closely packed on a hexagonal network (Koltover et al., 1998), another where positively charged vesicles attach to the extended DNA molecule, the so-called “beads on a string” model (Felgner et al., 1987; Gershon et al., 1993; Ruozi et al., 2007; Sternberg et al., 1994), and a final one where DNA is expected to collapse and attach in the form of a globule into the outer surface of positively charged vesicles (Miguel et al., 2003). What can be drawn from all four cases, whatever the nature of the interactions, is that at dilute concentrations no structural change in the systems is present, namely vesicle or bilayer disruption, whereas at high concentrations the situation becomes different with vesicles tending to disrupt and flocculate (Dias et al., 2002; Radler et al., 1997; Salditt et al., 1997;). Concerning polyplexes, rod-like, globular, and toroidal DNA condensates are the morphologies most commonly observed (Carnerup et al., 2009; Danielsen et al., 2004).

### 1.4.3 Binding affinity

The capability of lipo- and polyplexes to avoid premature dissociation and promote the release of genetic material to the cytoplasm once inside the cell is strongly related to the binding affinity between the DNA and the vector in question (Prevette et al., 2007). Indeed, a strong binding affinity between DNA and its carrier entails a high DNA compaction and protection against degradation in the extracellular environment. However, following their escape from endosomes, the complexes need to approach the nucleus, as well as dissociate; as such, a high DNA-vector binding affinity might constitute a limiting step for transfection considering the difficulty in the separation of the DNA from its gene carrier (Tros de Ilarduya et al., 2010). For the case of polyplexes, presenting by far the highest degree of DNA binding affinity (and condensation), it is well accepted that the molecular weight (Mw) of the polycation (directly related to the cationic valence) is a key factor controlling the DNA-vector binding affinity and subsequent transfection. In general, lower Mw polycations yield higher DNA transfection efficiencies (Ziady et al., 1999) as the DNA dissociation from them is faster (Schaffer et al., 2000).

## 2. Polycation-mediated gene delivery: Our main results

As already mentioned, the present chapter concerns with the physicochemical characterization of the DNA compaction and transfection mediated by polycations and cationic liposomes. Two families of polycations, Chitosan and Poly (diallyldimethylammonium chloride) (pDADMAC), and one cationic lipid formulation extensively used worldwide in transfection assays, Metafectene® Pro (MEP), are characterized as DNA vectors. Important for the DNA complexation, the structural, electrochemical, and energetic aspects are assessed. Particular attention is paid to the effect of polycations charge density and valence on complex parameters such as i) the hydrodynamic radius,  $R_H$ , ii) the stability with time, iii) the vector to DNA ratio at which complexation takes place, iv) the  $\zeta$ -potential, v) the energetics of binding, vi) the morphology, and vii) transfection efficiency.

It has to be noted that our characterizations were conducted as a function of two distinct cation-to-anion ratios reported in either molar (i.e., the N/P ratio, sections 2.1 and 2.2) or mass units (i.e., the L/D ratio, section 2.3). To get a complete description of the sample preparation, experimental procedures, and data analysis of the results here exposed, the reader is encouraged to consult our published papers (Alatorre-Meda et al., 2009; Alatorre-Meda et al., 2010a, 2010b; Alatorre-Meda et al., 2011). Outstanding results are presented below.

2.1 The DNA-chitosan system

Upon mixing, oppositely charged polyelectrolytes interact electrostatically and form complexes in a process that is promoted by an increase in entropy which is due to a release of counterions (Manning, 1978; Matulis et al., 2000). Accordingly, polycation molecular parameters such as charge density and valence have gained attention in recent reports (Danielsen et al., 2004; Maurstad et al., 2007).

The role of chitosan charge density is well established. It is accepted that the high charge density of chitosan at pHs below its pKa results beneficial for polyplex preparation, and also that its low charge density at pH 7.4 contributes to a low polyplex cytotoxicity and facilitates the intracellular release of DNA from the complex after its endocytotic cellular uptake (Strand et al., 2010). By contrast, the role of chitosan valence on transfection efficiency is contradictory. Namely, while several studies promote the use of high Mw chitosans (Huang et al., 2005; MacLaughlin et al., 1998), some other publications report that lower Mw chitosans are superior for gene transfer (Koping-Hoggard et al., 2003; Lavertu et al., 2006).

Aiming to draw general conclusions about the feasibility of using chitosan as a gene carrier, we characterized the DNA complexation and transfection mediated by three chitosans presenting different Mw (three different valences) at three different pHs of 5.0, 6.0, and 6.5 (three different charge densities). Table 1 summarizes the physical characteristics of the chitosans employed.

CHITOSAN	[ $\eta$ ] (dl g <sup>-1</sup> )	Mw (kDa)	Label
Low viscous	4.42 $\pm$ 0.01	111 $\pm$ 2	C(689)
Middle viscous	7.85 $\pm$ 0.24	266 $\pm$ 14	C(1652)
Highly viscous	11.40 $\pm$ 0.24	467 $\pm$ 18	C(2901)

Table 1. Chitosans employed.

2.1.1 Chitosan to DNA complexation ratio, (N/P)<sub>c</sub>

Stable DNA-chitosan polyplexes, ensuring a complete DNA compaction, are usually formed when chitosan is added in molar excess relative to the negatively charged DNA; however, excessive positive charges might lead to cytotoxicity since negatively charged cell membranes are prone to be damaged in the presence of cationic, extracellular compounds (Thomas & Klibanov, 2003). Consequently, finding a molar ratio exhibiting stable complexes at the lowest possible chitosan concentration becomes important. Such a concentration, presenting this mandatory characteristic, is what we define as the chitosan to DNA complexation ratio (N/P)<sub>c</sub>.

a. Determination of the  $(N/P)_c$  via static light scattering (SLS)

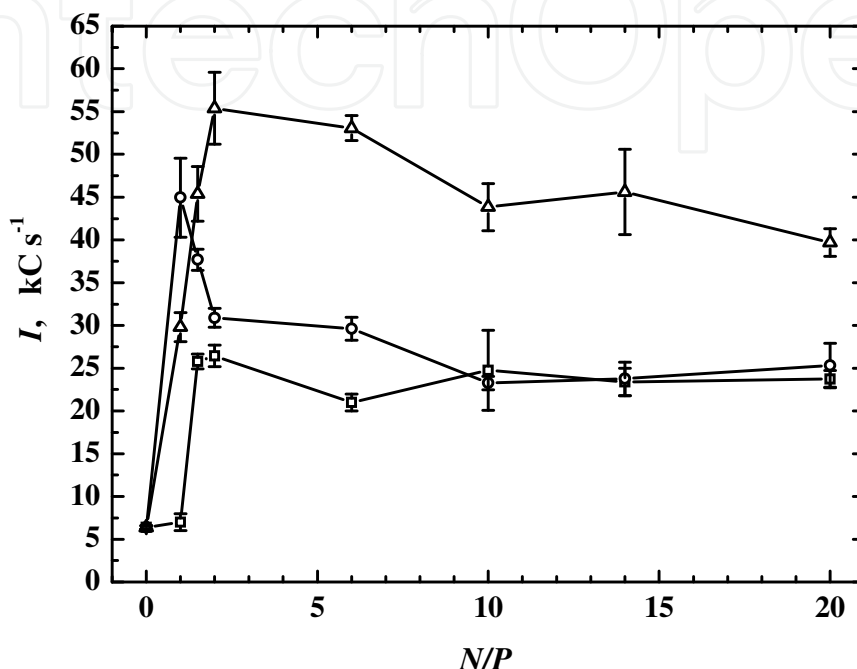
It is well accepted that linear, highly charged polyelectrolytes, at the dilute and semi-dilute regimes, can interact via a Coulombic repulsive potential which is strong enough to keep the polymer chains elongated and widely separated, although these interactions be partly screened by non-condensed counterions in solution (Manning, 1978). Polyelectrolytes in such concentration regimes produce in consequence very small scattering signals when irradiated with any source of light (Drifford & Dalbiez, 1984). The situation is rather distinct when polyelectrolytes interact one with each other or are complexed with external agents; in such a case they scatter higher amounts of light when irradiated (Drifford & Dalbiez, 1984). Based on these foundations we analyzed our polyplexes via SLS in order to follow the complexation process. SLS has proved to be a suitable tool to detect structural changes in linear biopolymers expected to be compacted provided that upon structural changes (such as the coil-globule transition observed during DNA compaction) they must scatter light to different extents.

To determine  $(N/P)_c$ , we tested numerous chitosan/DNA formulations with varying  $N/P$  ratios (at a constant DNA concentration) in terms of the chitosan charge density and valence. What we found by SLS was that there exist, indeed, a molar ratio from which the structural conformation of the polyplexes remains apparently constant independently of further addition of chitosan (i.e., presenting non-accentuated changes in light scattering intensity). That molar ratio, defined as  $(N/P)_c$ , proved to be strongly influenced by the chitosan charge density adopting values of around 1.5, 2.0, and 6.0 for the pHs of 5.0, 6.0, and 6.5, respectively. Our estimations, inferred from figure 1, can be discussed as follows.

Figure 1 presents the light scattering intensity of the DNA-C(1652) polyplexes as a function of the  $N/P$  ratio for the three studied pHs. This figure reflects various features worth analyzing. Interestingly, the system revealed plots similar in shape, but different in  $I$  values. The plots collected at pH 5.0 and 6.0 have  $I$  values one close to the other, whereas the plot at pH 6.5 has higher  $I$  values over the whole range of  $N/P$  studied. In all three plots three distinct regions can be identified, namely at  $N/P = 0$ , at  $0 < N/P \lesssim 2$ , and at  $N/P > 2$ . At  $N/P = 0$ , the system containing pure DNA shows the intensity at least five times lower than the samples at  $N/P > 2$ , indicating no aggregation. However, upon addition of chitosan to DNA, the intensity increases sharply with the maximum at  $N/P$  around 1-2 to finally level off at  $N/P > 2$ . This peculiar and interesting behavior observed when chitosan concentration in the system relative to DNA is around 1-2, is suggestive of the formation of some kind of complex structures between DNA and chitosan at this region, large in size, possibly aggregates that are responsible for the dispersion of higher amounts of light. Finally at  $N/P > 2$ , the intensity  $I$  reaches a constant value revealing the presence of well-formed, stable DNA-chitosan polyplexes with regular sizes. The  $N/P$  ratio marking the onset of the constant value in  $I$  is denoted as the  $(N/P)_c$ . Very importantly, these results suggest that as the pH of the medium increases larger amounts of chitosans are required to completely compact the given amount of DNA. This phenomenon can be explained by the fact that at pHs close to its  $pK_a$  (6.3–6.5), chitosan undergoes a decrease in its charge density due to the neutralization of its amino groups (Kumar et al., 2004), a feature that becomes even more pronounced for chitosans with higher molecular weights (higher valences) (MacLaughlin et al., 1998). Therefore, and having in mind that one of the driving forces of polyelectrolyte complexation is the release of counterions from the polyanion-polycation pair (Manning, 1978; Matulis et al., 2000), it is not strange that the binding affinity between DNA and chitosan lowered as the pH increased and got close to 6.5. Likewise, the highest intensities



observed for the system at pH 6.5 over the whole range of N/P can be attributed to a lower chitosan solubility (also ascribed to pHs close to the pKa), a fact that leads to the formation of polyplexes of sizes larger than those at lower pHs, as described below (MacLaughlin et al., 1998; Mumper et al., 1995). The DNA-C(689) and -C(2901) systems revealed the same behavior (data not included).



Adapted from (Alatorre-Meda et al., 2009).

Fig. 1.  $I$  vs.  $N/P$  of the DNA-C(1652) polyplexes at pH = 5.0 (squares), pH = 6.0 (circles), and pH = 6.5 (triangles).

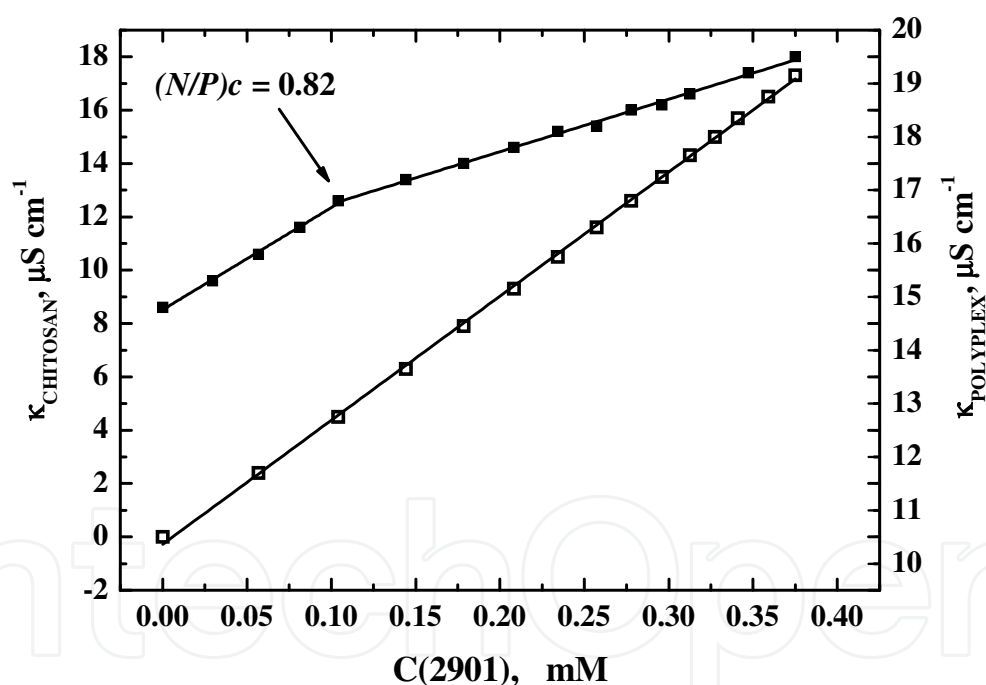
#### b. Determination of the $(N/P)_c$ by conductometry

Electrostatic interactions between oppositely charged polyelectrolytes entail a release of counterions (Manning, 1978; Matulis et al., 2000). The tracking of this release by means of conductometry can be employed as a tool to characterize the DNA compaction process (Rodriguez-Pulido et al., 2008). To confirm the  $(N/P)_c$  values obtained by SLS we measured the change in conductivity provoked by the addition of chitosan solutions to both, DNA and pure buffer solutions. Compared to those of SLS, the conductometry results, depicted in figure 2, reveal  $(N/P)_c$  values slightly lower. Main findings as well as a possible explanation to the observed differences are exposed below.

Figure 2 presents a representative plot of the electrical conductivity,  $\kappa$ , as a function of the polycation concentration, recorded for C(2901) at pH 5.0. The filled and empty squares stand for the DNA and pure buffer reservoir solutions, respectively. As can be seen from this figure, in the buffer solution alone the conductivity increased linearly with the chitosan concentration (empty squares) indicating that no aggregation took place under the whole range of the polycation concentration. In the DNA solution (filled squares) by contrast, the conductivity grew linearly, however, with a clear change in slope at the chitosan

concentration of 0.104 mM, corresponding to the N/P ratio of 0.82. A similar inflection in a conductivity plot during DNA compaction upon addition of a cationic vector has been observed elsewhere (Rodriguez-Pulido et al., 2008). The authors suggested that the increase in conductivity related to the counterion release from the polycation injected is accentuated by the release of counterions resulting from the complexation process (in our case  $\text{Na}^+$  from DNA and  $\text{CH}_3\text{COO}^-$  from chitosan) thereby justifying a higher slope in the conductivity plot below the inflection point. On the other hand, once the inflection occurred, the lower slope can be attributed to the fact that only the counterions coming from the chitosan dissociation now contribute to the conductivity of the solution. This change in slope of the conductivity plot can in consequence be considered as the point from which DNA is compacted, namely  $(\text{N/P})_c$  (Rodriguez-Pulido et al., 2008).

Compared to the DNA compaction ratio we determined by SLS ( $(\text{N/P})_c \sim 1.5$ ), the lower ratio of  $\text{N/P} = 0.82$  here depicted can be ascribed to the difference in ionic strength of the media used in both experiments and to the fact that contrary to SLS, in the conductometry experiment the complex formation was run at constant stirring.<sup>1</sup> The other two chitosans, C(689) and C(1652), although with slight differences in the conductivity values, revealed the inflection point at exactly the same N/P ratio as compared to C(2901) (plots not shown).



Reproduced from (Alatorre-Meda et al., 2011) with permission of Elsevier BV in the format Journal via Copyright Clearance Center.

Fig. 2. Electrical conductivity,  $\kappa$ , vs. C(2901) concentration. Filled and empty squares stand for the addition of chitosan to a DNA and to a pure buffer solution, respectively. (Note the difference in scales).

<sup>1</sup> Sample preparation for conductometry experiments is described in (Alatorre-Meda et al., 2011). To consult the experimental conditions for SLS go to (Alatorre-Meda et al., 2009).

### 2.1.2 Time stability and size

To determine the time stability of the polyplexes, we measured by dynamic light scattering (DLS) the hydrodynamic radius,  $R_H$ , of a sample presenting an  $N/P > (N/P)_c$  (more specifically,  $N/P = 6$ ) during a period of 6 days at the three different pHs of interest. In general, the polyplexes, regardless of charge density and valence, presented constant sizes with fluctuations lower than a 10% (data not shown). Thus, and provided that small fluctuations as those observed in our measurements are most likely related to the nature of the DLS technique, the polyplexes can be considered as stable with time.

Considering their time stability, to calculate the characteristic size of the polyplexes we simply averaged the  $R_H$  values obtained along the testing time. The polyplex sizes thereby obtained were in the range of  $187 \pm 21 < R_H < 246 \pm 13$  nm, in good agreement with results previously reported (Mumper et al., 1995). However, contrary to what we initially expected, the size of the polyplexes was found to be dependent on the chitosan valence, following a linear trend with the chitosan molecular weight.<sup>2</sup> Figure 3 depicts the average size of the polyplexes (regardless of chitosan charge density) as a function of the chitosan molecular weight.

Increasing trends in the complex size with polycation Mw, such as that observed in figure 3, are well documented in the literature. For the case of chitosan, it has been demonstrated that upon increasing in its chain length, the influence of the charge density with its correspondent entropy gain decrease. It is likely that the restriction of the polycation chain upon complexation becomes more important, giving rise to a different complexation behavior of high Mw chitosans compared to low Mw chitosans (Danielsen et al., 2004; Maurstad et al., 2007). Furthermore, the intuitive assumption that a higher Mw chitosan can interact better with DNA (due to its expected higher valence), and thus condense it more efficiently than a chitosan of a lower Mw is outweighed by the fact that a higher molecular weight chitosan is less soluble, and as a result, an increase in complex diameter or even complex aggregation may result (MacLaughlin et al., 1998; Mumper et al., 1995).

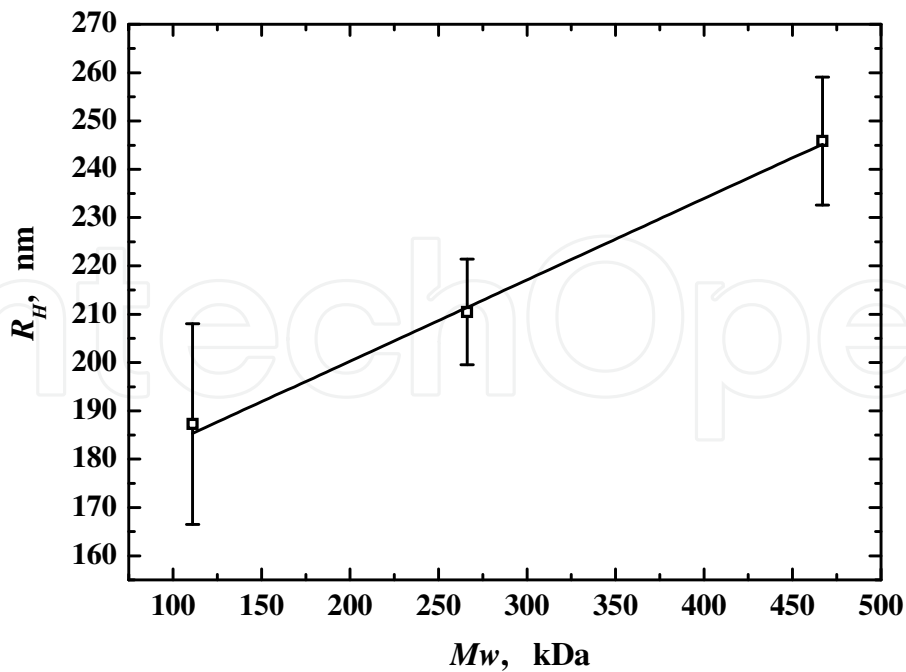
A general conclusion drawn throughout these sections is that an increased charge density of chitosan, resulting from a lowering of pH, leads to a greater binding affinity between chitosan and DNA as fewer chitosan is required to reach the complexation and the complexes thereby formed are more stable (Alatorre-Meda et al., 2009). Consequently, and in order to further understand the general aspects involved in the DNA-chitosan interactions, in subsequent studies we focused on working at acidic conditions exclusively (Alatorre-Meda et al., 2011). The influence of chitosan valence at those conditions on complex physicochemical properties other than size is described below.

### 2.1.3 Surface charge

For many polyplexes the cross-over from a negative to a positive  $\zeta$ -potential occurs at or very close to the isoneutrality point  $(N/P)_\phi$ .  $(N/P)_\phi$  is defined as the point at which the  $N/P$  ratio of the polyplex equals 1, that is, the ratio where the negative charges of DNA are stoichiometrically neutralized by the positive charges of the polycation (De Smedt et al., 2000).

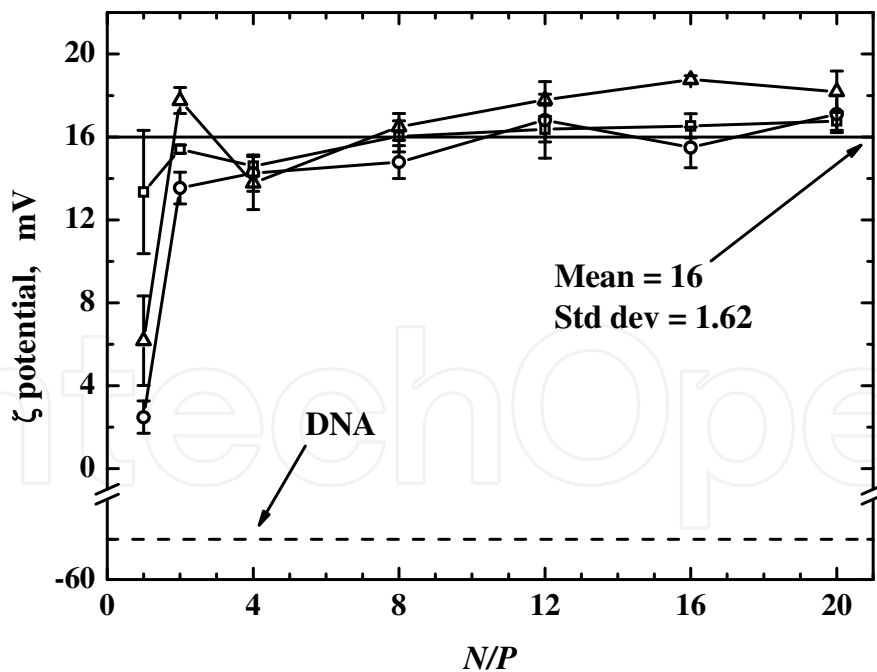
---

<sup>2</sup> In general, it is believed that polycations with higher charge densities and valences should produce smaller DNA complexes.



Reproduced from (Alatorre-Meda et al., 2009) with permission of Elsevier BV in the format Journal via Copyright Clearance Center.

Fig. 3.  $R_H$  of DNA-chitosan polyplexes, vs.  $M_w$  of chitosan.



Reproduced from (Alatorre-Meda et al., 2011) with permission of Elsevier BV in the format Journal via Copyright Clearance Center.

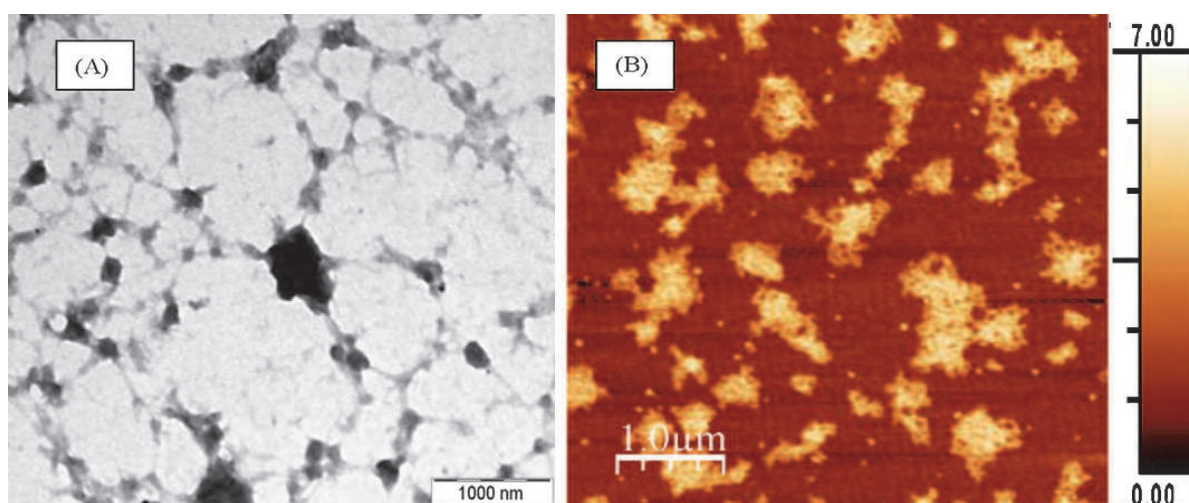
Fig. 4.  $\zeta$ -potential of DNA-chitosan polyplexes vs.  $N/P$ . DNA-C(689) (squares), DNA-C(1652) (circles), and DNA-C(2901) (triangles) are plotted. The dotted line stands for the DNA solution ( $\zeta$ -potential = -55 mV).

In the present study, the characterization was done in the range  $1 \leq N/P \leq 20$  for all polyplexes. The  $\zeta$ -potential of the polyplexes is plotted as a function of  $N/P$  in figure 4. In general, all polyplexes presented a positive, stable  $\zeta$ -potential from  $N/P$  ratios as low as  $(N/P)_c$  confirming that DNA is completely compacted independently of further addition of chitosan. Main findings can be discussed as follows.

It can be seen from figure 4 that at  $N/P = 1$  all polyplexes, in particular those formed with C(1652) and C(2901), reveal a lower  $\zeta$ -potential as compared to the rest of compositions. The cationic vector-mediated DNA coil to globule transition demonstrated by other authors (Dias et al., 2005) in conjunction with the base line-absent DLS correlation functions we obtained for these systems at ratios  $N/P \leq 1$  (Alatorre-Meda et al., 2009), may provide an explanation to this feature. Apparently, larger amounts of chitosan are needed to completely compact the DNA and in consequence populations entailing varying extents of DNA compaction are expected to be present in the bulk. On the other hand, at ratios higher than  $(N/P)_\phi$ , all polyplexes reach a plateau around 16mV regardless of chitosan Mw, which is in good agreement with other DNA-polycation systems (Tang & Szoka, 1997). This positive  $\zeta$ -potential of the polyplexes suggests that the DNA compaction is completely achieved with chitosan chains probably pointing to the outer part of the polyplexes as inferred by other authors (Koping-Hoggard et al., 2003).

#### 2.1.4 Structural organization

Imaging techniques can detect, localize, and analyze individual aggregates of a heterogeneous population, thereby revealing events that would otherwise be hidden. In this context transmission electron- and atomic force microscopy (TEM and AFM) are frequently used in parallel for the visual characterization of biological molecules (Arakawa et al., 1992; Lin & Goh, 2002). Figure 5 presents typical TEM (A) and AFM (B) images obtained for the DNA-C(689) polyplexes at  $N/P = 20$ . This figure reflects that the polyplexes adopt a peculiar brush-like conformation in which DNA is apparently confined to the interior of the complex although not fully compacted. The reason why of this polyplex conformation as well as the implications it might have on transfection are discussed below.



Reproduced from (Alatorre-Meda et al., 2011) with permission of Elsevier BV in the format Journal via Copyright Clearance Center.

Fig. 5. TEM (A) and height AFM (B) images of DNA-C(689) polyplexes,  $N/P = 20$ . The bar next to (B) represents the Z scale in nm.

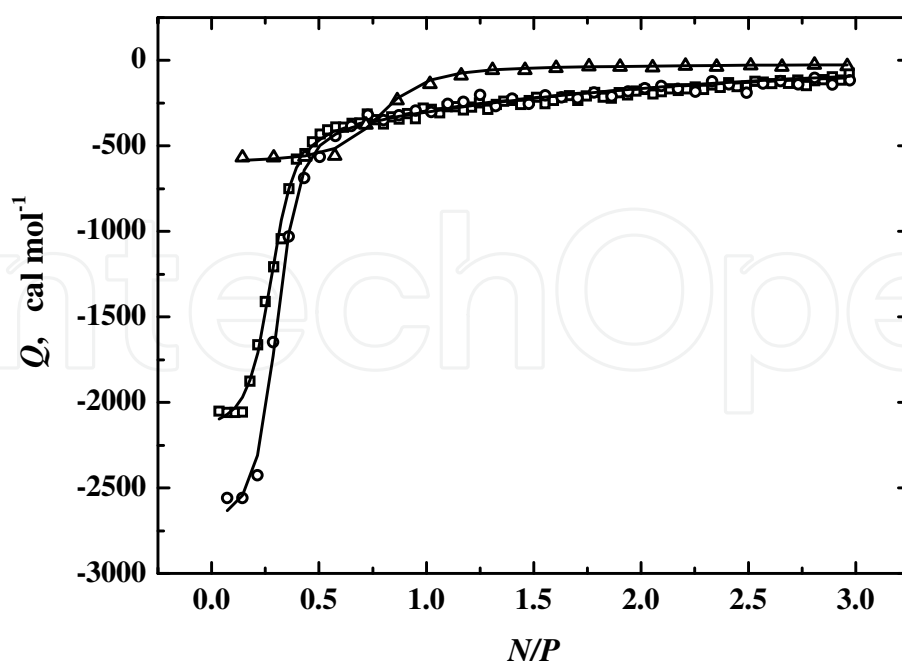


It has been reported that the DNA complexation with chitosans might result in a blend of structures: toroids, rods, and globules, with the relative amounts of the different structures apparently depending on the actual chitosan, the charge ratio, and solution properties like pH and ionic strength (Danielsen et al., 2004; Maurstad et al. 2007). What we observe from figure 5A and B is a heterogeneous population of polyplexes with particle sizes ranging from 250 to 500 nm in good agreement with the DLS results (see section 2.1.2). Both images depict polyplexes with a brush-like conformation where globules/aggregates comprise a dense core that is surrounded by a “hairy” shell of polymer chains. This globular conformation has been reported as characteristic of the DNA complexation with high molecular weight chitosans ( $M_w > 100$  kDa) (Danielsen et al., 2004; Maurstad et al., 2007); by contrast, complexes formed with lower molecular weight chitosans adopt toroid- and rod-like conformations (Maurstad et al., 2007). Similar brush-like structures were also obtained for the DNA complexation with transferrin-poly(l-lysine) conjugates. In this case, the complex morphology was found to depend on the conjugate to DNA ratio (Wagner et al., 1991). Carnerup and coworkers suggest that the significant morphological rearrangement undergone by DNA when it is condensed with low  $M_w$  polycations is because of the low charge density of the polycation in question (Carnerup et al., 2009). For toroidal aggregates to form, the electrostatic attraction has to be moderate; that is, a balance between mobility and high binding affinity of DNA to the polymer has to exist. In such a system, the condensed DNA chains will be able to arrange into a toroid. On the contrary, if the charge density of the polymer is too high (as expected for chitosan at pH 5), the DNA chains will entangle with the polymer ones, forming globular aggregates (Carnerup et al., 2009). Therefore, provided that our polyplexes proved to be stable (see section 2.1.2), the “not so tight” DNA complexation they present should be beneficial for DNA transfection (Tros de Ilarduya et al., 2010).

Very importantly, the morphological structure of our system depicted by TEM and AFM in conjunction with the markedly positive  $\zeta$ -potentials obtained for the polyplexes at this high N/P ratio (see the previous section) appear to be in line with the core-shell structure proposed for polycation-excessive DNA complexes (A. V. Kabanov & V. A. Kabanov, 1998). This model states that DNA is condensed in the inner part of the polyplex by the binding of short segments of a large number of polycation chains, whereas the remaining segments of these same chains are expected to be free in the outer part of the polyplexes giving rise to markedly positive polyplex surface charges (A. V. Kabanov & V. A. Kabanov, 1998).

### 2.1.5 Binding affinity and complexation thermodynamics

Once the complex is released from the endosome, DNA must disassemble from its vector to be accessible to the cell machinery responsible for translating the enclosed information. For the case of polyplexes, the DNA decompaction (disassembly) is a process substantially dependent on i) the DNA-vector binding affinity, ii) the complexation thermodynamics, and iii) the solution conditions (Carlstedt et al., 2010; Prevettte et al., 2007). Provided that acidic conditions demonstrated to be optimal for polyplex formation (see previous sections), we evaluated the DNA-chitosan binding affinity and complexation thermodynamics at a solution pH of 5.0. As depicted by isothermal titration calorimetry (ITC), lower valence chitosans demonstrated to have a higher binding affinity for DNA. Main results are described below.



Reproduced from (Alatorre-Meda, et al., 2011) with permission of Elsevier BV in the format Journal via Copyright Clearance Center.

Fig. 6. Integrated heat of interaction of the titration of chitosan to DNA vs. N/P. Chitosans C(689) (squares), C(1652) (circles), and C(2901) (triangles) were titrated. Solid lines represent the two site model fitting to the experimental data.

Figure 6 shows the heat of interaction resulting from the titration of chitosan to DNA as a function of N/P. Supported on calorimetric measurements, it is well accepted that polyelectrolyte complex formation and coacervation are mainly entropically driven through the release of condensed counterions via the ion-exchange process in which an endothermic signal is recorded during the complex formation (de Kruif et al., 2004; Matulis et al., 2000). By contrast, in a result most commonly observed in the formation of protein-ligand complexes, it can be observed from figure 6 that for all experiments the injection of chitosan appears as a markedly negative signal at the beginning of the binding process followed by a gradual decrease in the released heat up until thermal equilibrium, that is, the complexation is exothermic. A similar decrease in the quantity of heat released on successive injections of titrant has been interpreted as an indicative of the progressive neutralization of charges in the reservoir molecule; meanwhile, the zone of the thermogram in which a plateau in the heat released is reached might be attributed to the complete DNA compaction (Bharadwaj et al., 2006). In this context, comparing the onset of the plateau yielded for the three chitosans during the DNA compaction it is clear that for C(2901)  $N/P \sim 1$ , whereas for C(689) and C(1652)  $N/P \sim 0.5$ . This result is consistent with those we observed by SLS (section 2.1.1) and  $\zeta$ -potential (previous section) indicating that the use of higher valence chitosans, even at low pHs, apparently demands larger amounts of cationic polymer for DNA compaction. This is also supported by the 4–5-fold smaller enthalpic contribution rendered by C(2901) compared to its lower valence homologues (discussed below).

Table 2 summarizes the enthalpy, entropy, binding constant, and the stoichiometry of the DNA–chitosan interaction derived from the data fitting of figure 6.

chitosan	$K_1 \times 10^{-5}$ (M <sup>-1</sup> )	$n_1$	$\Delta H_1$ (kcal mol <sup>-1</sup> )	$\Delta S_1$ (kcal mol <sup>-1</sup> K <sup>-1</sup> )
C(689)	29.9 ± 0.75	0.27 ± 0.03	-2.176 ± 0.23	0.022
C(1652)	29.0 ± 1.23	0.27 ± 0.05	-2.712 ± 0.12	0.020
C(2901)	4.82 ± 0.08	0.73 ± 0.01	-0.598 ± 0.07	0.024
chitosan	$K_2 \times 10^{-5}$ (M <sup>-1</sup> )	$n_2$	$\Delta H_2$ (kcal mol <sup>-1</sup> )	$\Delta S_2$ (kcal mol <sup>-1</sup> K <sup>-1</sup> )
C(689)	0.095 ± 0.01	0.86 ± 0.02	-1.304 ± 0.16	0.014
C(1652)	0.011 ± 0.02	0.75 ± 0.04	-1.357 ± 0.12	0.014
C(2901)	0.009 ± 0.01	0.62 ± 0.07	-0.529 ± 0.02	0.012

Reproduced from (Alatorre-Meda et al., 2011) with permission of Elsevier BV in the format Journal via Copyright Clearance Center.

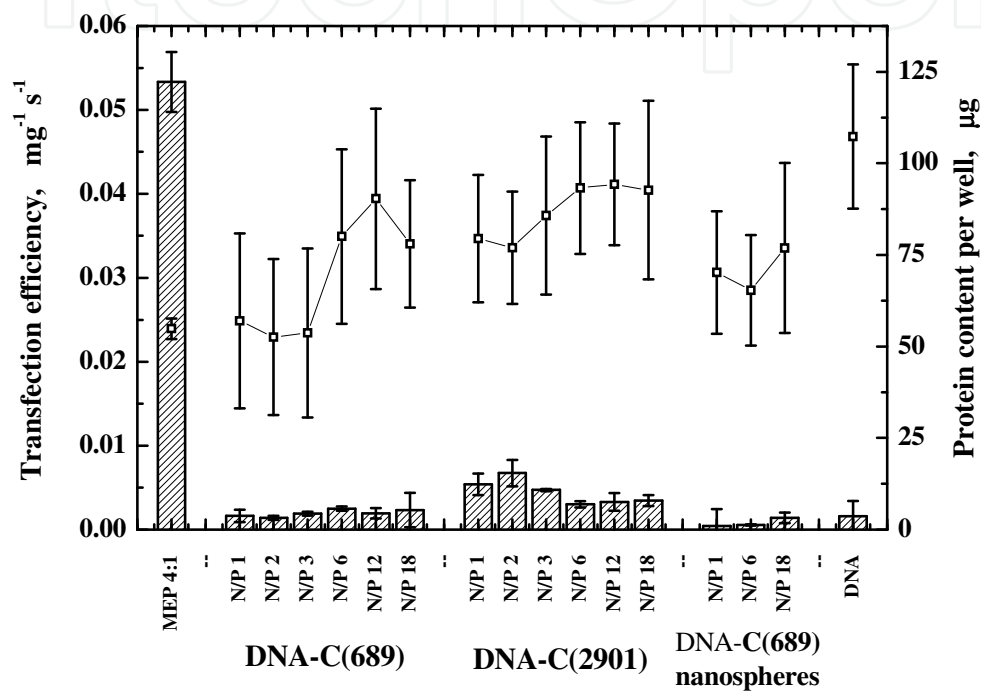
Table 2. Thermodynamic parameters of the DNA-chitosan binding process. Sub-indices next to each parameter stand for the corresponding sites 1 and 2.

As can be observed from this table, the DNA binding constants obtained for all chitosans are on the order of 10<sup>5</sup> to 10<sup>6</sup> and 10<sup>3</sup> to 10<sup>4</sup> M<sup>-1</sup> for the first and second class of binding sites, respectively. These results are in good agreement with previously reported values for other systems including cationic polymers (Nisha et al., 2004; Prevette, et al., 2007) and proteins (Engler et al., 1997; Milev et al., 2005). On the other hand, the decreasing values of the binding constants with the chitosan valence reveal that lower valence chitosans have a higher binding affinity for DNA. This is indicative that chitosan chains may undergo steric restrictions as Mw (valence) increases, restrictions that in turn apparently hamper the interpolyelectrolyte interactions (Danielsen et al., 2004; Maurstad et al., 2007). Concerning the enthalpy, it is well known that it results from a combination of electrostatics, conformational changes (especially for second binding sites), and hydrogen bonding interactions; therefore, ΔH cannot be strictly related to any one contribution. However, and despite the experimental evidence demonstrating that the binding enthalpy ΔH was negative, the DNA–chitosan complexation was proved to be entropically driven. This result is in good agreement with other electrostatic, polyelectrolyte associations promoted by the release of counterions and solvent upon attraction (Matulis et al., 2000; Prevette, et al., 2007; Srinivasachari et al., 2007).

2.1.6 Transfection efficiency

The potential of chitosans C(689) and C(2901) as DNA carriers towards HeLa cells was evaluated. Polyplexes and nanospheres with compositions in the range 1 ≤ N/P ≤ 18 were tested. In addition, a MEP:DNA lipoplex (4:1 μL:μg) and naked DNA were measured as positive and negative controls, respectively. Although considerably lower compared to that of the DNA–MEP lipoplex, the transfection efficiency of the polyplexes was found to increase with chitosan valence as depicted by the β-galactosidase and luciferase expression assays. Main findings are described below.

Figure 7 shows the transfection efficiency of the polyplexes and controls as well as the protein content of the wells after lysis. Two features are observed from this figure. On the one hand, it is clear that polyplexes within the whole range of ratios rendered levels of  $\beta$ -galactosidase expression slightly higher than that of the negative control (DNA without polymer) with transfection efficiency being increased with chitosan valence. This result is somehow logical taking into account the lower binding affinity depicted by ITC assays for the DNA-C(2901) complex (see Table 2); that is, the DNA release from this complex in the interior of the cell is expected to be favored. On the other hand, compared to that of the DNA-MEP lipoplex, the transfection efficiency of the polyplexes is considerably lower.



Reproduced from (Alatorre-Meda et al., 2011) with permission of Elsevier BV in the format Journal via Copyright Clearance Center.

Fig. 7. Transfection efficiency of the DNA-chitosan complexes (columns) and protein content in wells after lysis (squares) vs. N/P.

Speculating that the low transfer rate of the polyplexes (compared to that of the lipoplex) might be related to cytotoxicity effects, the protein concentration was determined via the BCA assay. From figure 7 (right hand side axis) a comparable level of protein content for all formulations including the blanks was observed. Even if not totally conclusive regarding a measure of the cytotoxicity, this result shows that the cells proliferated approximately in the same way; consequently, the poor transfection efficiency shown by the DNA-chitosan polyplexes cannot be ascribed to cytotoxicity.

In the light of the transfection efficiency depicted by the polyplexes, a second kind of experiment was implemented. DNA-chitosan nanospheres were prepared following the protocol described by Mao and coworkers (Mao et al., 2001). The transfection efficiency results for C(689) are also plotted in figure 7. Compared to the polyplexes, no transfection improvement was observed, on the contrary, nanospheres in general showed a decreasing in gene expression yielding results only comparable to the naked DNA administration.

The luciferase assay was conducted in order to confirm the results obtained by the  $\beta$ -galactosidase assay. The transfection efficiency for all cases was similar to that observed in the  $\beta$ -galactosidase method. In general, naked DNA and complexes regardless of the N/P ratio and structure yielded a luminescence three orders of magnitude lower than that of the DNA-MEP lipoplex. Concerning the protein content determined by the BCA assay, the polyplexes and nanospheres rendered protein contents slightly higher than that of the DNA-MEP lipoplex (data not shown). In consequence, the transfection efficiency of polyplexes was confirmed to be low compared to that of the lipoplex.

In general, the low capacity of DNA to escape from complexes is regarded as one of the major limitations for the transfection efficiency of polyplexes (Midoux et al., 2009; Tros de Ilarduya et al., 2010). This feature has been ascribed to a number of factors. While some authors support that an excess of polycation, even in the presence of chloroquine, limits the protein expression due to *in vitro* cytotoxicity (Fischer et al., 2004), other authors affirm that the low tolerance of DNA to dissociate from polyplexes is presumably due to the bulky form they adopt in solution (Izumrudov et al., 1999). In our case the low transfection efficiency of the DNA-chitosan polyplexes compared to that of the lipoplex is most likely related to both the colloidal properties they exhibit and the DNA-chitosan binding affinity. On the one hand, the morphological structure depicted by TEM and AFM in conjunction with the markedly positive  $\zeta$ -potentials obtained suggest a core-shell like polyplex structure with chitosan occupying the outer part of the complex (A. V. Kabanov & V. A. Kabanov, 1998). On the other hand, as mentioned before, chitosans presenting higher DNA binding affinities were found to yield lower transfection efficiencies.

### 2.1.7 Particular conclusions

In general, the DNA-chitosan polyplexes exhibited good colloidal properties such as sizes in the range of 180 to 250 nm,  $\zeta$ -potentials of about 16 mV, and a stable core-shell like structural conformation. The influence of chitosan charge density and valence on all these physicochemical properties can be summarized as follows.

#### 1. Role of chitosan charge density.

Chitosan charge density was found to play an important role on the complexation of DNA. Namely, as the solution pH got close to the chitosan pKa, the neutralization of the amino groups, entailing a decrease of chitosan charge density, resulted in a higher amount of chitosan needed for complexation. That is, the acidic conditions were found to be favorable for complex formation.

#### 2. Role of chitosan valence.

Chitosan valence was found to be related to both the polyplex size and, more importantly, to the transfection efficiency. On the one hand, the hydrodynamic radii of complexes increased linearly with the chitosan Mw demonstrating that larger chitosan chains produce bulkier and less soluble polyplexes. On the other hand, in what we conceive as the main contribution of our investigations, we found that higher valence chitosans, exhibiting lower DNA binding affinities, yielded higher DNA transfection efficiencies.

## 2.2 The DNA-pDADMAC system

As stated before, cationic polymers most commonly studied as gene carriers include chitosan, PEI, PLL, poly( $\beta$ -amino ester)s, and poly-(amidoamine) dendrimers. In addition,



because of its permanent cationic charge, poly(diallyldimethylammonium chloride) (pDADMAC) has recently been explored as well (Fischer et al., 2004; Krajcik et al., 2008). pDADMAC is a water soluble cationic polymer. It is composed of mainly configurational isomers of pyrrolidinium rings and a small amount of pendant double bonds (Dautzenberg et al., 1998; Jaeger et al., 1996). With the pendent allylic double bonds being less reactive than those of the monomer, strictly linear macromolecules are formed at low conversions, but branching can proceed at high conversions as was demonstrated for commercial samples (Wandrey et al., 1999). Because of its physical structure pDADMAC is a highly flexible polymer compared to other polycations such as chitosan (Marcelo et al., 2005; Trzcinski et al., 2002). pDADMAC has been widely used in technical applications as a flocculant agent and as a composite for biosensors, which is because of its pH-independent cationic charge (Dautzenberg et al., 1998; Jaeger et al., 1996).

	Mw (kDa)	Label
Homopolymers	< 100	p(1, < 619)
	150	p(1, 929)
	275	p(1, 1703)
	450	p(1, 2786)
Copolymer	250	p(0.26, 668)

Table 3. pDADMACs employed. In p(x,y), x and y stand for charge density and valence, respectively.

In the present section we summarize outstanding results obtained in our laboratory describing relevant physicochemical characteristics of the DNA-pDADMAC complexes (Alatorre-Meda et al., 2010b). As done for chitosan in the previous section, we highlight the role of pDADMAC charge density and valence. Four homo-polymers (charge density = 1, with different valences) and one co-polymer, p(acrylamide-co-diallyldimethylammonium chloride) (coDADMAC) (charge density < 1, equivalent in valence to one of the homopolymers), were employed. Table 3 lists the cationic polymers characterized as gene carriers along with the nomenclature cited throughout this section.

2.2.1 DNA-pDADMAC characteristic ratios, (N/P)c and (N/P)\*

Different to the chitosan system, the DNA-pDADMAC polyplexes exhibited two distinct characteristic ratios: the previously observed (N/P)c (i.e., the ratio from which DNA is compacted) and (N/P)\*, an additional ratio from which the polyplexes adopt the most compact structure. Similarly to the DNA-chitosan polyplexes, (N/P)c was found to be dependent on the polycationic charge density, whereas (N/P)\* proved to be a function of pDADMAC valence. Table 4 summarizes the characteristic ratios for each DNA-pDADMAC system together with the average size of the polyplexes formed (discussed in the next section). Our main findings can be described as follows.

(N/P)c was determined by means of conductometry. pDADMAC aliquots were injected to DNA and buffer solutions and the change in conductivity was recorded. Successive pDADMAC injections produced exactly the same outcome observed for the chitosan system; namely, a linear increment in conductivity for the buffer solution and an inflection

in the conductivity plot for the DNA one (plots not shown). The ratio at which the conductivity inflection occurred is reported as (N/P)<sub>c</sub> (see section 2.1.1 for a complete explanation).

It is clear from table 4 that (N/P)<sub>c</sub> is governed by the charge density provided that polyplexes formed with pDADMAC homopolymers have complexation ratios lower than that of the polyplex formed with coDADMAC. This result confirms what we observed for chitosan not only with respect to the role of charge density but also regarding the (N/P)<sub>c</sub> values obtained which are very similar for both chitosan- and pDADMAC-based polyplexes (see section 2.1.1).

polymer	(N/P) <sub>c</sub>	(N/P)*	R <sub>H</sub> (nm)
p(1, < 619)	0.7	4	79.4 + 2.1
p(1, 929)	0.6	2	87.0 + 6.9
p(1, 1703)	0.7	2	108.9 + 12.5
p(1, 2786)	0.6	1	112.6 + 9.7
p(0.26, 668)	1.5	2	199.8 + 23.5

Reproduced from (Alatorre-Meda et al., 2010b) with permission of AMERICAN CHEMICAL SOCIETY in the format Journal via Copyright Clearance Center.

Table 4. Characteristic N/P ratios and R<sub>H</sub> of the DNA-pDADMAC polyplexes. (N/P)<sub>c</sub> and (N/P)\* stand for the DNA compaction ratio (determined by conductometry) and for the ratio from which the size of the polyplexes remain constant (determined by DLS), respectively. R<sub>H</sub> is the average of the recorded values in the range (N/P)\* ≤ N/P ≤ 10.

(N/P)\* was found by DLS as a characteristic ratio from which the polyplexes adopt the most compact structure. As observed from table 4, the value of (N/P)\* follows a decreasing trend with pDADMAC valence of the polyplexes, with p(1,619) and p(1,2786) showing the highest and the lowest (N/P)\* values of 4 and 1, respectively. The interplay between (N/P)<sub>c</sub> and (N/P)\* can be reasoned in terms of the different complexation states of DNA mediated by pDADMAC (Fischer et al., 2004).

2.2.2 Time stability and size

The characterization of the DNA-pDADMAC polyplexes in terms of size and time stability was carried out by means of DLS. The study was done in two steps. First, the hydrodynamic radii of the polyplexes, R<sub>H</sub>, were determined at 0.2 ≤ N/P ≤ 10. And second, the evolution of R<sub>H</sub> with time was followed for the polyplexes at N/P = 10. R<sub>H</sub> results are depicted in table 4. It is observed from table 4, that similarly to the chitosan systems, the size of the polyplexes was found to increase with pDADMAC valence, that is, the general assumption that the electrostatic interactions are outweighed to a certain extent by a decrease in the polycation solubility is confirmed (MacLaughlin et al., 1998; Mumper et al., 1995). Concerning the coDADMAC polyplex, it is clear that its size is ca. twice as big as those of the pDADMAC polyplexes. This outcome can be a consequence of an expected lower degree of DNA

compaction provided that the amount of positive charges in the polycation chain is lower, as also demonstrated for other systems encompassing non-ionic copolymers grafted to polycationic segments (Toncheva et al., 1998). Alternatively, the high hydrophilic capacity of acrylamide (AM) (Nuno-Donlucas et al., 2004) may allow larger amounts of water to be housed in the complex interior, resulting in bulkier polyplexes.

On the other hand, the time stability of the DNA-pDADMAC polyplexes was measured by following the time evolution of  $R_H$  for polyplexes at an N/P ratio of 10, as mentioned before. We observed that the sizes of the polyplexes formed with lower valence polymers remained practically constant during 7 days (ca. 85 nm). However, contrary to what we found with the chitosan systems, the DNA-p(1, 1703), -p(1, 2786), and -p(0.26, 668) polyplexes, whose initial sizes were above 100 nm, apparently underwent a structural change with time, resulting in a size reduction (data not shown). This structural rearrangement appeared to be valence-dependent since for the DNA-p(1,1703) system the size stabilization occurred from day 2 on, while for the DNA-p(1,2786) one it occurred from day 3 on. In general, it is theorized that both the branching of the pDADMAC polymer chain, expected to be present in a large extent (Wandrey et al., 1999), and the low stiffness of pDADMAC (Jaeger et al., 1989) are the main causes of such a behavior. Anyway, the final sizes of the homopolymer- and copolymer-based complexes were of ca. 85 and 120 nm, respectively.

2.2.3 Surface charge

In the present study, the  $\zeta$ -potential characterization was done in the range  $0.2 \leq N/P \leq 10$  for all polyplexes. Results are summarized in table 5. All polyplexes presented a positive, stable  $\zeta$ -potential from N/P ratios as low as (N/P)<sub>c</sub>. As concluded for chitosan complexes, this result suggests a complete DNA compaction. Main findings are discussed below.

N/P	p(1, < 619)	p(1, 929)	p(1, 1703)	p(1, 2786)	p(0.26, 668)
0.2	-45.0 + 3.2	-44.3 + 1.9	-43.1 + 0.7	-39.9 + 3.0	-41.4 + 2.3
0.4	-44.6 + 1.4	-33.3 + 1.4	-35.4 + 2.2	-41.2 + 3.5	-35.5 + 1.3
0.6	-35.3 + 1.4	-34.3 + 3.5	-33.6 + 2.0	-40.6 + 1.3	-34.0 + 6.0
0.8	-29.0 + 5.5	-24.0 + 5.4	-16.4 + 12.0	-22.3 + 2.6	-24.0 + 1.6
1	7.7 + 0.8	10.5 + 0.8	10.1 + 0.5	11.8 + 1.1	-19.9 + 1.9
2	11.8 + 0.7	12.2 + 0.1	11.2 + 0.4	11.8 + 0.6	12.7 + 0.3
4	11.7 + 1.3	10.5 + 0.8	13.1 + 0.6	12.0 + 0.7	11.5 + 0.2
6	12.2 + 0.5	12.0 + 0.5	12.0 + 0.3	11.9 + 0.3	10.6 + 0.5
10	11.8 + 0.3	12.0 + 0.3	11.9 + 0.4	12.8 + 0.1	12.3 + 0.1

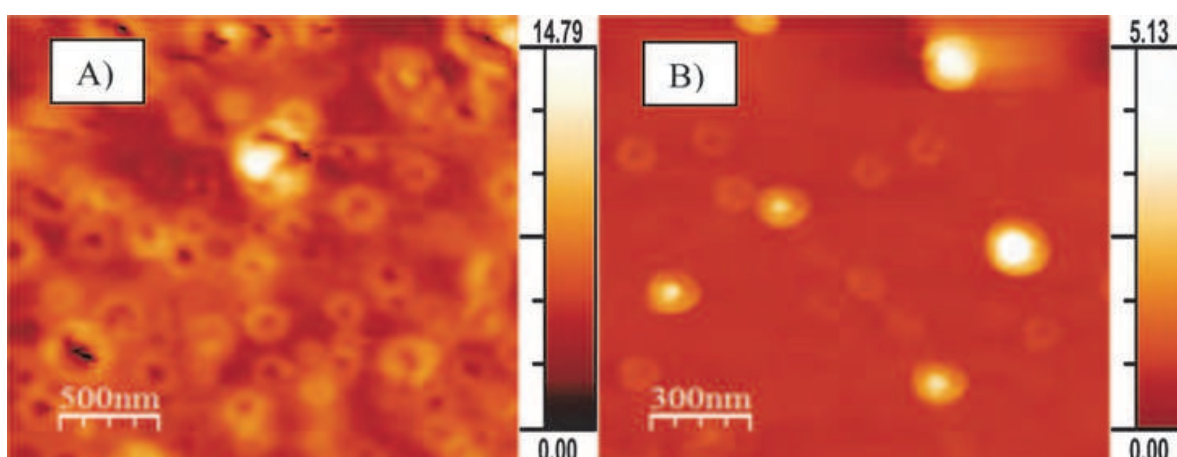
Reproduced from (Alatorre-Meda et al., 2010b) with permission of AMERICAN CHEMICAL SOCIETY in the format Journal via Copyright Clearance Center.

Table 5.  $\zeta$ -potential of the DNA-pDADMAC polyplexes (in mV) measured at different N/P ratios.

The data in table 5 reveal that all polyplexes, regardless of pDADMAC valence, present a constant  $\zeta$ -potential value of around 12 mV at  $N/P > (N/P)_c$ , which is in good agreement with the chitosan systems. Of special interest for gene therapy is the fact that the presence of AM, expected to improve the polyplex biocompatibility, does not cause a decrease in the positive charge recommended for transfection. Very importantly, these constant  $\zeta$ -potential values, irrespective of further addition of pDADMAC, are also suggestive of a polyplex core-shell conformation, as observed for the chitosan-mediated complexes (see section 2.1.3).

#### 2.2.4 Structural organization

In order to illustrate the morphology of the polyplexes, tapping mode AFM in air was conducted. Figure 8 shows images of DNA polyplexes made with p(0.26, 668) (A), and with p(1, 2786) (B) at a constant ratio  $N/P = 10$ .



Reproduced from (Alatorre-Meda et al., 2010b) with permission of AMERICAN CHEMICAL SOCIETY in the format Journal via Copyright Clearance Center.

Fig. 8. Height AFM images of DNA polyplexes made with p(0.26, 668) (A), and with p(1, 2786) (B) at  $N/P = 10$ . Bars next to images represent the Z scale in nm.

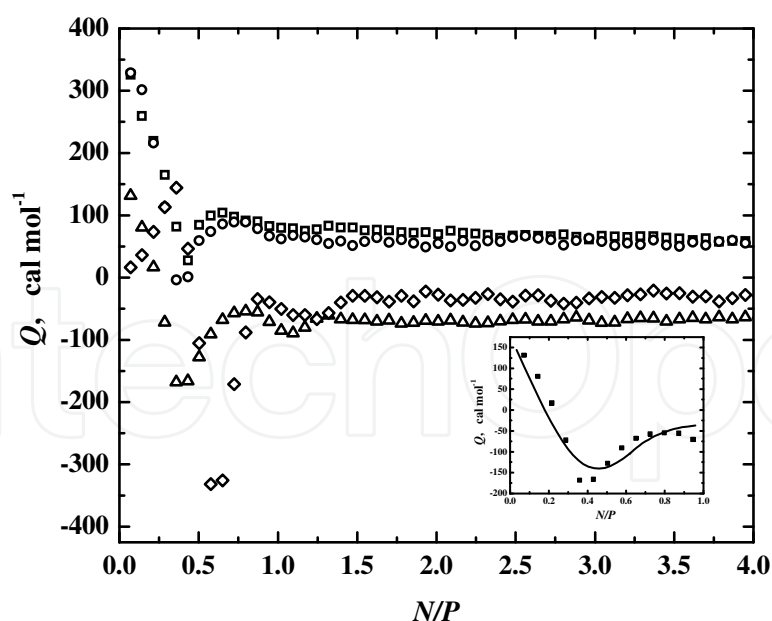
Both figures depict high populations of well-defined toroids with sizes ranging from 125 to 250 nm and 80 to 200 nm for the DNA-p(0.26, 668) and the -p(1, 2786) polyplexes, respectively. As mentioned before, the toroidal conformation suggests a maximum DNA compaction. For the case of the pDADMAC polyplexes, this maximum DNA compaction seems logical given the permanent cationic charge of the polymer; however, for the case of the coDADMAC polyplex, such a high DNA compaction appears to be somehow counterintuitive in view of the fact that three molecules of non-ionic AM are present per each molecule of cationic charged DADMAC (Alatorre-Meda et al., 2010b). Concerning the smaller sizes depicted by AFM as compared to those displayed by DLS, it should be recalled that for the former technique the samples were dried before the measurement, that is, polyplexes apparently became dehydrated.

#### 2.2.5 Binding affinity and complexation thermodynamics

As done for the DNA-chitosan polyplexes, ITC was performed to evaluate the DNA-pDADMAC binding affinity and complexation thermodynamics. Striking results were obtained as compared to the chitosan systems. Firstly, the DNA binding affinity of pDADMACs was found to be favored with valence; secondly, the complexation process was completed in three successive stages. Main results are discussed below.

Figure 9 shows the heat of interaction resulting from the titration of pDADMACs to DNA as a function of N/P. Three consecutive processes along the DNA-pDADMAC binding are observed. The first phase of binding occurred at N/P molar ratios lower than  $\sim 1$ , drawing a biphasic nature of the binding profiles for all polymers (except for p(1,<619)). As the polymer chains began to saturate the DNA, the slightly endothermic binding enthalpy decreased and reached an exothermic minimum at an N/P ratio of  $\sim 0.5$ . Similar slight endothermic heats have been ascribed to entropy-driven binding processes (Matulis et al., 2000; Srinivasachari et al., 2007) and ligand interactions with the DNA minor groove (Privalov et al., 2007). Concerning the reduction in the heat of interaction  $Q$ , it might result from the combination of both a decreased accessibility of binding sites to polymer molecules due to partial saturation of DNA molecules and from the dipole-dipole interactions between water molecules oriented favorably on adjacent DNA and polymer molecules (Strey et al., 1998). At this stage, bending of single DNA strand, bridging of neighboring DNA molecules by polymer chains and hydration can contribute to DNA collapse (Rau & Parsegian, 1992).

The second phase of binding was characterized by an additional post-transition endothermic heat which finished in a maximum for pDADMACs at an N/P molar ratio of  $\sim 0.75$ , with a subsequent decrease in enthalpy due to phosphate saturation. This endothermic heat increment with a subsequent peak or discontinuity has been suggested to represent the DNA collapse (Matulis et al., 2000). The increase in  $Q$ , from the zone in which DNA chains are partially saturated (the exothermic minimum) up to the observed maximum before phosphate saturation, is attributed to a binding of further polymer molecules to the partially saturated DNA. Finally, the third phase of binding was characterized by exothermic post-transition heats after complete phosphate saturation.



Reproduced from (Alatorre-Meda et al., 2010b) with permission of AMERICAN CHEMICAL SOCIETY in the format Journal via Copyright Clearance Center.

Fig. 9. Integrated heats of interaction of the titration of pDADMAC to DNA vs. N/P. Polymers p(1, <619) squares, p(1, 919) circles, p(1,1703) triangles, and p(1, 2786) diamonds were employed. The solid line in the inset represents the data fitting of the DNA-p(1, 1703) interaction.



Table 6 summarizes the enthalpy, entropy, binding constant, and the stoichiometry of the DNA–pDADMAC interaction derived from the data fitting of figure 9.

polymer	$K_1 \times 10^{-5}$ (M <sup>-1</sup> )	$n_1$	$\Delta H_1$ (kcal mol <sup>-1</sup> )	$\Delta S_1$ (kcal mol <sup>-1</sup> K <sup>-1</sup> )
p(1, < 619)	1.02 ± 0.26	0.44 ± 0.12	0.26 ± 0.07	0.023
p(1, 929)	3.10 ± 0.48	0.39 ± 0.11	0.20 ± 0.07	0.026
p(1, 1703)	51.6 ± 0.31	0.28 ± 0.07	0.07 ± 0.01	0.030
p(1, 2786)	55.1 ± 0.26	0.28 ± 0.07	0.06 ± 0.01	0.031
p(0.26, 668)	1.72 ± 0.14	0.86 ± 0.13	0.17 ± 0.03	0.024
polymer	$K_2 \times 10^{-5}$ (M <sup>-1</sup> )	$n_2$	$\Delta H_2$ (kcal mol <sup>-1</sup> )	$\Delta S_2$ (kcal mol <sup>-1</sup> K <sup>-1</sup> )
p(1, < 619)	0.06 ± 0.04	0.33 ± 0.10	2.34 ± 1.86	0.020
p(1, 929)	0.12 ± 0.07	0.26 ± 0.10	0.92 ± 0.74	0.022
p(1, 1703)	0.42 ± 0.08	0.15 ± 0.06	-0.40 ± 0.11	0.019
p(1, 2786)	0.43 ± 0.07	0.16 ± 0.06	-0.39 ± 0.11	0.020
p(0.26, 668)	0.17 ± 0.04	0.24 ± 0.04	-0.81 ± 0.07	0.020

Reproduced from (Alatorre-Meda et al., 2010b) with permission of AMERICAN CHEMICAL SOCIETY in the format Journal via Copyright Clearance Center.

Table 6. Thermodynamic parameters of the DNA-pDADMAC binding process. Sub-indices next to each parameter stand for the corresponding sites 1 and 2.

It can be observed from this table that the DNA binding constants obtained for all pDADMACs are on the order of 10<sup>5</sup>-10<sup>6</sup> and 10<sup>3</sup>-10<sup>4</sup> M<sup>-1</sup> for the first and second class of binding sites, respectively. These global ranges are in good agreement with the DNA-chitosan binding data; however, it is clear that the present case exhibits an opposite behavior regarding the DNA binding affinity, namely, it increases with the polycationic valence. This opposite trend might be ascribed to the high water solubility of pDADMAC. That is, although higher valence pDADMACs produced bulkier polyplexes (see section 2.2.2), it appears that the ion-pair electrostatic interactions are not hindered at all by steric restrictions (see sections 2.1.1 and 2.1.5). On the other hand, concerning the energetic implications, the DNA binding with all polymers showed slight enthalpic contributions in both sites. This outcome depicts an entropically driven reaction typically observed in polyelectrolyte associations (Matulis et al., 2000; Prevettte et al., 2007; Srinivasachari et al., 2007) where less favourable (more endothermic) ΔH values might be associated with breaking hydrogen bonds between polymer and water molecules (breaking a hydrogen bond in water corresponds to an enthalpy increase of 1.9 kcal/mol) (Silverstein et al., 2000).

2.2.6 Transfection efficiency

To determine the transfection efficiency of the DNA-pDADMAC polyplexes, we performed exactly the same protocols as those described for the chitosan systems (see section 2.1.6). Similarly to the chitosan complexes, the transfer rate of the pDADMAC polyplexes was very low compared to that of the DNA-MEP lipoplex. Even worse, polyplexes within the whole range of ratios rendered levels of β-galactosidase and luciferase expressions comparable to that of naked DNA (data not shown). Given that no cytotoxic effects can be argued

(Alatorre-Meda et al., 2010b), the low transfection efficiency demonstrated by pDADMAC (even lower than that of chitosan) might be ascribed to i) the polycation barrier occurring in the core-shell structure proposed (see section 2.1.4), ii) the high binding affinity depicted by ITC (high binding constants), and iii) the high degree of DNA compaction exhibited by the polyplexes (see sections 2.2.1 and 2.2.4).

### 2.2.7 Particular conclusions

In this section we described our most important findings regarding the characterization of pDADMAC as DNA carrier. In general, the DNA-pDADMAC polyplexes exhibited good colloidal properties such as sizes in the range of 80 to 200 nm,  $\zeta$ -potentials of about 12 mV, and stable toroidal structural conformations. However, the transfection efficiency was found to be even lower than that of the DNA-chitosan complexes. The influence of pDADMAC charge density and valence on the physicochemical properties of the polyplexes can be summarized as follows.

#### 1. Role of pDADMAC charge density.

pDADMAC charge density was found to play an important role on the DNA complexation ratio, (N/P)<sub>c</sub>. Our experiments demonstrated that the (N/P)<sub>c</sub> of pDADMACs polyplexes (pDADMAC charge density = 1) are lower than half the (N/P)<sub>c</sub> of the coDADMAC polyplex (coDADMAC charge density < 1).

#### 2. Role of pDADMAC valence.

pDADMAC valence was found to increase i) the size of the polyplexes, ii) the ratio from which the sizes remain practically constant, (N/P)\*, and iii) the DNA-pDADMAC binding affinity. In general, it is well accepted that higher valence polycations produce bulkier DNA polyplexes because of steric restrictions and solubility drops, giving support to our DLS results. However, our results demonstrate that the high water solubility and permanent cationic charge of pDADMAC apparently compensate such restrictions giving rise to higher binding affinities and lower (N/P)\* ratios as the valence increases. Such high DNA-pDADMAC interactions proved to reduce the transfection efficiency (at least compared to the chitosan-mediated complexes). Finally, in what time stability concerns, higher valence pDADMACs were found to provoke a polyplex size reduction with time. This structural rearrangement may be related to both the branching of the pDADMAC polymer chain, expected to be present in a large extent, and the low stiffness of pDADMAC.

### 2.3 The DNA-MEP system

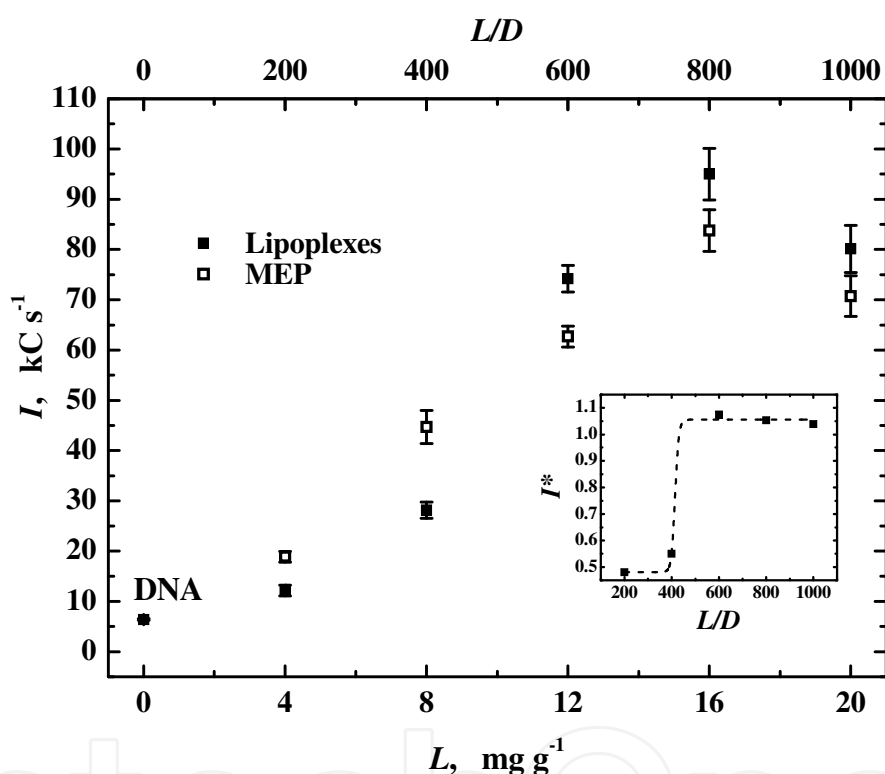
Metafectene® Pro (MEP) is a liposomal formulation that encompasses a mixture of a polyamine-lipid as the cationic group (average molecular weight of the repeat unit of 272.26 g mol<sup>-1</sup>) and DOPE as the helper lipid. It belongs to a new class of transfection reagents based on the Repulsive Membrane Acidolysis technology (RMA) developed by Biontex laboratories GmbH (Bonetta 2005). Based on its high efficiency as transfection vector toward eukaryotic cells (Aluigi et al., 2007; Ibrahim & Kim, 2008; Kwon & Kim, 2008; Spinosa et al., 2008), MEP has been routinely used in our laboratories as a positive blank for DNA transfection assays. As observed in previous sections, compared to polyplexes formed with polycations chitosan and pDADMAC, the DNA-MEP lipoplexes yielded transfection rates markedly higher; therefore, it was of our interest to characterize the DNA-MEP complexation process from a physicochemical point of view attempting to elucidate the reason why of such a big difference in the transfection efficiencies.

The present section details the physical chemistry characterization of the interactions of MEP with DNA around the mass ratio recommended for transfection (L/D ~ 700). Aiming

to establish a more general conclusion about the DNA-polyelectrolyte interactions, the experimental conditions implemented (salt concentration in buffer, pH, and temperature) were chosen to be similar to the other systems previously studied (Alatorre-Meda et al., 2010a). For simplicity and in order to use units consistent with the protocols established for transfection, all characterizations presented in this section are expressed in terms of the liposome to DNA mass ratio,  $L/D$ . Main results are exposed below.

### 2.3.1 MEP to DNA complexation ratio, $(L/D)_c$

As done for chitosan polyplexes, the DNA-MEP complex formation was addressed via SLS. Depicted by a sharp increase in the scattering intensity, we determined the complexation ratio as  $(L/D)_c \sim 600$ . Our main findings are described below.



Reproduced from (Alatorre-Meda et al., 2010a) by permission of the PCCP Owner Societies.

Fig. 10. Average intensity of light scattered,  $I$ , by lipoplexes (filled squares) and by MEP (empty squares) as a function of the mass ratio  $L/D$ , and of the concentration  $L$ , respectively. The average intensity of light scattered by DNA is also included. The inset shows the average intensity scattered by lipoplexes normalized to the sum of the intensities scattered by MEP and by DNA in separate. The dotted line is a guide for the eye.

Figure 10 depicts the average intensity of the light scattered by lipoplexes as a function of the mass ratio  $L/D$ , and by MEP solutions in absence of DNA as a function of the concentration  $L$ . This figure shows that at  $L/D \sim 600$  the intensity of light scattered by lipoplexes is roughly 50% lower than that scattered by their corresponding MEP solutions, whereas for  $(L/D) \geq 600$  this trend shifts, becoming higher the intensities scattered by the lipoplexes. An increment like this in the light scattered was observed along the DNA-

chitosan complexation process (see section 2.1.1). In that case, the increment in the scattering was attributed to the change in the particle structure, where the intensity of light scattered by the collapsed polymeric chains was confirmed to be higher than that scattered by the linear chains of DNA and chitosan before mixing. Nevertheless, in the present case the hydrodynamic radius of MEP scarcely changed after its mixing with DNA (see the following section), suggesting no change either in its vesicular conformation or in the coil conformation of DNA. Therefore, in our opinion the increase in intensity in the zone of  $L/D \geq 600$  can only be explained in terms of a constructive interference that presumably arises when liposomes are connected one to each other by DNA coils (see section 2.3.4), where contrary to moving freely they start to move in ensemble. This assumption becomes clearer when the normalized intensity of the lipoplexes, ( $I^* = I_{\text{lipoplex}} / (I_{\text{DNA}} + I_{\text{MEP}})$ ), is plotted as a function of the mass ratios (inset in Fig. 10).

The inset shows two well differentiated regions, one for  $L/D < 600$  where DNA and MEP are expected not to interact, and other for  $(L/D) \geq 600$  where, in good agreement with the zone suggested by Biontex Laboratories GmbH and demonstrated by transfection assays (Aluigi, et al., 2007; Ibrahim & Kim, 2008; Kwon & Kim, 2008; Spinoso et al., 2008), complexation occurs. On the other hand, the lowest intensity exhibited by pure DNA, as aforementioned, is a behavior characteristic of linear molecules in solution which are hardly detected by SLS (Drifford & Dalbiez, 1984).

### 2.3.2 Size and time stability

Particle sizes of both MEP and lipoplexes were measured via DLS in order to be compared. We found that the size of the MEP vesicles was equivalent to that of the lipoplexes, with the latter ones being slightly smaller (ca. 135 nm). It appears then, that as DNA comes in contact with MEP, the polyanion acts as a stabilizer of the liposomes, a result that has been observed for other polymer-vesicle interactions (Antunes et al., 2009; Rodriguez-Pulido et al., 2008). Very importantly, compared to the other DNA-cationic vector formulations here studied, in particular to the DNA-chitosan system ( $R_H$  up to 450 nm), the sizes depicted by the DNA-MEP complexes are considerably lower. This is believed to facilitate the cellular uptake (Tros de Ilarduya, et al., 2010).

To check the stability of the lipoplexes, we measured the time evolution of  $R_H$  of samples with  $L/D \geq (L/D)_c$ . The magnitude of  $R_H$  during the testing time (7 days) changed less than a 10% in all cases, with the mean value and standard deviation lowering as the value of  $L/D$  increased (data not shown). Thus, the lipoplexes were validated as stable.

### 2.3.3 Surface charge

In order to elucidate the lipoplex charge at the transfection conditions, we studied the  $\zeta$ -potential of the lipoplexes around the mass ratio recommended for transfection. To our surprise, the  $\zeta$ -potential of the lipoplexes at the transfection conditions resulted to be negative (data not shown). This striking result finds support on the lipoplex structural conformation we detected by TEM and AFM (see next section) showing non-complexed DNA segments. Alternatively, as reported by others (Dias et al., 2002; Radler et al., 1997; Salditt et al., 1997), there must be a coexistence of DNA and lipoplexes in which, provided the negative  $\zeta$ -potential, DNA is expected to be in excess.

Compared to cationic lipoplexes, negatively charged ones should offer advantages of decreased cytotoxicity and increased serum compatibility (Thakor et al., 2009); however, as

mentioned before, their cell internalization is problematic. Cell internalization of negatively charged particles often requires the presence of cell-specific ligands (attached to particle surface) for endocytosis to occur. Such ligands build the “bridge” between cellular membranes and particles otherwise absent in view of the electrostatic repulsions (Kono et al., 2001; Sahay et al., 2010; Simoes et al., 1998). By contrast, anionic particles not bearing cell-specific ligands are expected to enter cells during mitosis<sup>3</sup> (Khalil et al., 2006).

#### 2.3.4 Structural organization

Figure 11 presents typical TEM (A and B) and AFM (C and D) images obtained for lipoplexes at L/D = 1000. This figure depicts non aggregated liposomes with DNA coils coming out from their surfaces seemingly connecting them; a feature that is more easily observed in the zooms shown in panels B and D. Such a morphology, referred to as the “beads on a string” conformation, has been observed not only for DNA-vesicle systems but also for DNA-micellar aggregates (Ruozi et al., 2007; Wang et al., 2007). In general, this structural conformation, occurring at low lipid to DNA ratios, is believed to appear because of packing and bending constraints on the long DNA molecules (Dan, 1998). Of importance for gene therapy, the exposed DNA sections are covered by a metastable, cylindrical lipid bilayer that protects DNA from inactivation or degradation (Sternberg et al., 1994).

#### 2.3.5 Transfection efficiency

As observed in previous sections, compared to polyplexes formed with polycations chitosan and pDADMAC, the DNA-MEP lipoplex yielded transfection rates markedly higher. We speculate that the higher transfection efficiency of the MEP lipoplex must be related to a successful endosomal escape that is promoted simultaneously by a repulsive membrane acidolysis process and different conformational transitions adopted by DOPE upon pH changes (Bonetta 2005; Khalil et al., 2006; Tros de Ilarduya et al., 2010). Concerning the cell entrance mechanism our lipoplexes should display, we hypothesize mitosis as the most probable option given both the negative  $\zeta$ -potential of the system and that, to our best knowledge, MEP does not contain any kind of cell-receptors. In this context, HeLa cells (the cells we worked with) are recognized as highly proliferating ones (Ota, et al., 2010). Importantly, as part of our protocols we seeded the cells at an 80-90% optical confluence so that transfection was practiced with the maximum possible number of healthy cells, assuring mitosis.<sup>4</sup>

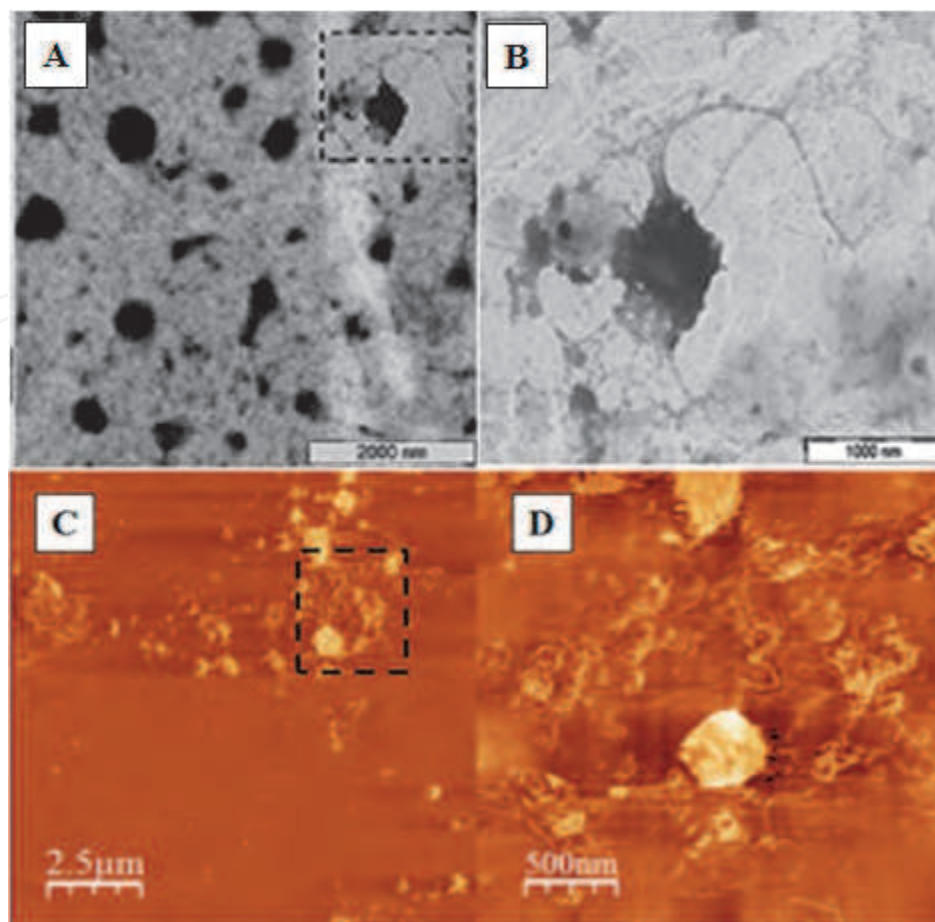
#### 2.3.6 Particular conclusions

Emphasizing the importance of studying the lipoplex formation under the same conditions at which transfection is practiced, our results point to a “beads on a string” complex conformation as depicted by i) the TEM and AFM micrographs revealing coils of DNA coming out from vesicle surface, ii) the  $\zeta$ -potential results showing that the transfection mass ratios are well below isoneutrality, and iii) the practically constant vesicle sizes after complexation depicted by DLS. On the other hand, a sharp increase in the intensity of light

<sup>3</sup> Mitosis is also accepted as an important factor in the nuclear translocation of transgenes given that the integrity of the nuclear membrane is transiently lost, allowing their entrance (Khalil et al, 2006).

<sup>4</sup> It has to be noted that this very reasoning should be applied to the chitosan- and pDADMAC-mediated polyplexes.





Reproduced from (Alatorre-Meda et al., 2010a) by permission of the PCCP Owner Societies.

Fig. 11. Typical TEM (A and B) and AFM (C and D) images obtained for DNA-MEP lipoplexes at  $L/D = 1000$ .

scattered by samples marks  $(L/D)_c \sim 600$  as the zone from which lipoplexes exist, validating the mass ratio recommended for transfection of  $(L/D) \sim 700$ . Finally, DLS results reveal lipoplexes with an average size of 135 nm that were stable within at least 7 days.

### 3. General conclusions and forthcoming work

In general, the DNA-chitosan and DNA-pDADMAC systems revealed good colloidal properties and similar physicochemical features as compared one to each other. They were able to condense DNA plasmids to form particles small and positive enough so as to be taken up to cells by endocytosis; however, the transfection efficiency they rendered was markedly lower than that of the DNA-MEP lipoplex. With the experimental results here presented it appears that this low transfection efficiency relies on the high DNA-polycation binding affinity coupled with the structural conformation the polyplexes adopt in solution. Additionally, repulsive membrane acidolysis processes and different conformational transitions adopted by DOPE upon pH changes confer the MEP lipoplex a successful endosomal escape not occurring during polyplex transfection.

In light of the obtained results a deeper understanding of both the complex internalization to cells and DNA release from complexes to the cytoplasm must, in our opinion, be achieved

in order to improve the transfection process. In the context of the DNA release, special attention needs be paid to the development of strategies assuring a high degree of DNA-vector de-compaction. Interesting pioneering results stem from publications by González-Pérez and coworkers (Carlstedt et al., 2010; Gonzalez-Perez & Dias, 2009; Gonzalez-Perez et al., 2008).

#### 4. Acknowledgment

M. A.-M. thanks the Ramón Areces foundation for his Post-Doctoral fellowship (Research project: 2010/CL509).

#### 5. References

- Alatorre-Meda, M.; González-Pérez, A. & Rodríguez, J. R. (2010). "DNA-Metafectene™ PRO complexation: A physical chemistry study. *Phys. Chem. Chem. Phys.*, Vol. 12, No. 27, (July 2010), pp. 7464-7472, ISSN 1463-9076.
- Alatorre-Meda, M.; Taboada, P.; Hartl, F.; Wagner, T.; Freis, M. & Rodríguez, J. R. (2011). The influence of chitosan valence on the complexation and transfection of DNA: The weaker the DNA-chitosan binding the higher the transfection efficiency. *Colloids and Surfaces B: Biointerfaces*, Vol. 82, No. 1, (January 2011), pp. 54-62, ISSN 0927-7765.
- Alatorre-Meda, M.; Taboada, P.; Krajewska, B.; Willemeit, M.; Deml, A.; Klösel, R. & Rodríguez, J. R. (2010). DNA-Poly(diallyldimethylammonium chloride) complexation and transfection efficiency. *J. Phys. Chem. B*, Vol. 114, No. 29, (July 2010), pp. 9356-9366, ISSN 1520-6106.
- Alatorre-Meda, M.; Taboada, P.; Sabin, J.; Krajewska, B.; Varela, L. M. & Rodríguez, J. R. (2009). DNA-chitosan complexation: A dynamic light scattering study. *Colloids and Surfaces A: Physicochemical and Engineering Aspects*, Vol. 339, No. 1-3, (May 2009), pp. 145-152, ISSN 0927-7757.
- Aluigi, M. G.; Hofreiter, S.; Falugi, C.; Pestarino, M. & Candiani, S. (2007). Efficiency of two different transfection reagents for use with human NTERA2 cells. *European Journal of Histochemistry*, Vol. 51, No. 4, (October 2007), pp. 301-304, ISSN 1121-760X.
- Anderson, W. F. (1990). September 14, 1990: The beginning. *Human Gene Therapy*, Vol. 1, No. 4, (n.d. 1990), pp. 371-372, ISSN 1043-0342.
- Antunes, F. E.; Marques, E. F.; Miguel, M. G. & Lindman, B. (2009). Polymer-vesicle association. *Advances in Colloid and Interface Science*, Vol. 147-48, No. Sp. Iss. SI, (March 2009), pp. 18-35, ISSN 0001-8686.
- Arakawa, H.; Umemura, K. & Ikai, A. (1992). Protein images obtained by STM, AFM and TEM. *Nature*, Vol. 358, No. 6382, (July 1992) pp. 171-&, ISSN 0028-0836.
- Battersby, B. J.; Grimm, R.; Huebner, S. & Cevc, G. (1998). Evidence for three-dimensional interlayer correlations in cationic lipid-DNA complexes as observed by cryo-electron microscopy. *Biochimica Et Biophysica Acta: Biomembranes*, Vol. 1372, No. 2, (July 1998), pp. 379-383, ISSN 0005-2736.
- Behr, J. P. (1997). The proton sponge: A trick to enter cells the viruses did not exploit. *Chimia*, Vol. 51, No. 1-2, (January 1997), pp. 34-36, ISSN 0009-4293.
- Bharadwaj, S.; Montazeri, R. & Haynie, D. T. (2006). Direct determination of the thermodynamics of polyelectrolyte complexation and implications thereof for

- electrostatic layer-by-layer assembly of multilayer films. *Langmuir*, Vol. 22, No. 14, (July 2006), pp. 6093-6101, ISSN 0743-7463.
- Bloomfield, V. A. (1997). DNA condensation by multivalent cations. *Biopolymers*, Vol. 44, No. 3, (n.d. 1997), pp. 269-282, ISSN 0006-3525.
- Bonetta, L. (2005). The inside scoop-evaluating gene delivery methods. *Nature Methods*, Vol. 2, No. 11, (November 2005), pp. 875+, ISSN 1548-7091.
- Boussif, O.; Lezoualch, F.; Zanta, M. A.; Mergny, M. D.; Scherman, D.; Demeneix, B. & Behr, J. P. (1995). A versatile vector for gene and oligonucleotide transfer into cells in culture and in-vivo: polyethylenimine. *PNAS*, Vol. 92, No. 16, (August 1995), pp. 7297-7301, ISSN 0027-8424.
- Carlstedt, J.; Gonzalez-Perez, A.; Alatorre-Meda, M.; Dias, R. S. & Lindman, B. (2010). Release of DNA from surfactant complexes induced by 2-hydroxypropyl-beta-cyclodextrin. *International Journal of Biological Macromolecules*, Vol. 46, No. 2, (March 2010), pp. 153-158, ISSN 0141-8130.
- Carnerup, A. M.; Ainalem, M. L.; Alfredsson, V. & Nylander, T. (2009). Watching DNA condensation induced by poly(amido amine) dendrimers with Time-Resolved Cryo-TEM. *Langmuir*, Vol. 25, No. 21, (November 2009), pp. 12466-12470, ISSN 0743-7463.
- Dan, N. (1998). The structure of DNA complexes with cationic liposomes: cylindrical or flat bilayers? *Biochimica Et Biophysica Acta: Biomembranes*, Vol. 1369, No. 1, (February 1998), pp. 34-38, ISSN 0005-2736.
- Danielsen, S.; Varum, K. M. & Stokke, B. T. (2004). Structural analysis of chitosan mediated DNA condensation by AFM: Influence of chitosan molecular parameters. *Biomacromolecules*, Vol. 5, No. 3, (May 2004), pp. 928-936, ISSN 1525-7797.
- Dautzenberg, H.; Gornitz, E. & Jaeger, W. (1998). Synthesis and characterization of poly(diallyldimethylammonium chloride) in a broad range of molecular weight. *Macromolecular Chemistry and Physics*, Vol. 199, No. 8, (August 1998), pp. 1561-1571, ISSN 1022-1352.
- de Kruif, C. G.; Weinbreck, F. & de Vries, R. (2004). Complex coacervation of proteins and anionic polysaccharides. *Current Opinion in Colloid & Interface Science*, Vol. 9, No. 5, (December 2004), pp. 340-349, ISSN 1359-0294.
- De Smedt, S. C.; Demeester, J. & Hennink, W. E. (2000). Cationic polymer based gene delivery systems. *Pharmaceutical Research*, Vol. 17, No. 2, (February 2000), pp. 113-126, ISSN 0724-8741.
- Dias, R. S.; Innerlohinger, J.; Glatter, O.; Miguel, M. G. & Lindman, B. (2005). Coil-globule transition of DNA molecules induced by cationic surfactants: A dynamic light scattering study. *J. Phys. Chem. B*, Vol. 109, No. 20, (May 2005), pp. 10458-10463, ISSN 1520-6106.
- Dias, R. S.; Lindman, B. & Miguel, M. G. (2002). DNA interaction with cationic vesicles. *J. Phys. Chem. B*, Vol. 106, No. 48, (December 2002), pp. 12600-12607, ISSN 1520-6106.
- Dias, R. S.; Pais, A. A. C. C.; Miguel, M. G. & Lindman, B. (2003). Modeling of DNA compaction by polycations. *Journal of Chemical Physics*, Vol. 119, No. 15, (October 2003), pp. 8150-8157, ISSN 0021-9606.
- Dowty, M. E.; Williams, P.; Zhang, G. F.; Hagstrom, J. E. & Wolff, J. A. (1995). Plasmid DNA entry into postmitotic nuclei of primary rat myotubes. *PNAS*, Vol. 92, No. 10, (May 1995), pp. 4572-4576, ISSN 0027-8424.

- Drifford, M. & Dalbiez, J. P. (1984). Light-scattering by dilute-solutions of salt-free polyelectrolytes. *Journal of Physical Chemistry*, Vol. 88, No. 22, (n.d. 1984), pp. 5368-5375, ISSN 0022-3654.
- Engler, L. E.; Welch, K. K. & JenJacobson, L. (1997). Specific binding by EcoRV endonuclease to its DNA recognition site GATATC. *Journal of Molecular Biology*, Vol. 269, No. 1, (May 1997), pp. 82-101, ISSN 0022-2836.
- Felgner, P. L.; Gadek, T. R.; Holm, M.; Roman, R.; Chan, H. W.; Wenz, M.; Northrop, J. P.; Ringold, G. M. & Danielsen, M. (1987). Lipofection: A highly efficient, lipid-mediated DNA-transfection procedure. *PNAS*, Vol. 84, No. 21, (November 1987), pp. 7413-7417, ISSN 0027-8424.
- Fischer, D.; Dautzenberg, H.; Kunath, K. & Kissel, T. (2004). Poly(diallyldimethylammonium chlorides) and their N-methyl-N-vinylacetamide copolymer-based DNA-polyplexes: Role of molecular weight and charge density in complex formation, stability, and in vitro activity. *International Journal of Pharmaceutics*, Vol. 280, No. 1-2, (August 2004), pp. 253-269, ISSN 0378-5173.
- Gershon, H.; Ghirlando, R.; Guttman, S. B. & Minsky, A. (1993). Mode of formation and structural features of DNA cationic liposome complexes used for transfection. *Biochemistry*, Vol. 32, No. 28, (July 1993), pp. 7143-7151, ISSN 0006-2960.
- Gonzalez-Perez, A. & Dias, R. S. (2009). Different strategies for controlling DNA conformation: Compaction and decompaction. *FBS*, Vol. E1, (June 2009), pp. 228-241, ISSN 1945-0494.
- Gonzalez-Perez, A.; Dias, R. S.; Nylander, T. & Lindman, B. (2008). Cyclodextrin-surfactant complex: A new route in DNA decompaction. *Biomacromolecules*, Vol. 9, No. 3, (March 2008), pp. 772-775, ISSN 1525-7797.
- Haensler, J. & Szoka, F. C. (1993). Polyamidoamine cascade polymers mediate efficient transfection of cells in culture. *Bioconjugate Chemistry*, Vol. 4, No. 5, (September 1993), pp. 372-379, ISSN 1043-1802.
- Huang, M.; Fong, C. W.; Khor, E. & Lim, L. Y. (2005). Transfection efficiency of chitosan vectors: Effect of polymer molecular weight and degree of deacetylation. *Journal of Controlled Release*, Vol. 106, No. 3, (September 2005), pp. 391-406, ISSN 0168-3659.
- Ibrahim, A. M. A. & Kim, Y. (2008). Transient expression of protein tyrosine phosphatases encoded in Cotesia plutellae bracovirus inhibits insect cellular immune responses. *Naturwissenschaften*, Vol. 95, No. 1, (January 2008), pp. 25-32, ISSN 0028-1042.
- Izumrudov, V. A.; Zhiryakova, M. V. & Kudaibergenov, S. E. (1999). Controllable stability of DNA-containing polyelectrolyte complexes in water-salt solutions. *Biopolymers*, Vol. 52, No. 2, (n.d. 1999), pp. 94-108, ISSN 0006-3525.
- Jaeger, W.; Gohlke, U.; Hahn, M.; Wandrey, C. & Dietrich, K. (1989). Synthesis and application of flocculating agents. *Acta Polymerica*, Vol. 40, No. 3, (March 1989), pp. 161-170, ISSN 0323-7648.
- Jaeger, W.; Hahn, M.; Lieske, A.; Zimmermann, A. & Brand, F. (1996). Polymerization of water soluble cationic vinyl monomers. *Macromolecular Symposia*, Vol. 111, (December 1996), pp. 95-106, ISSN 1022-1360.
- Kabanov, A. V. & Kabanov, V. A. (1998). Interpolyelectrolyte and block ionomer complexes for gene delivery: Physicochemical aspects. *Advanced Drug Delivery Reviews*, Vol. 30, No. 1-3, (March 1998), pp. 49-60, ISSN 0169-409X.



- Ke, J. H. & Young T. H. (2010). Multilayered polyplexes with the endosomal buffering polycation in the core and the cell uptake-favorable polycation in the outer layer for enhanced gene delivery. *Biomaterials*, Vol. 31, No. 35, (December 2010), pp. 9366-9372, ISSN 0142-9612.
- Khalil, I. A.; Kogure, K.; Akita, H. & Harashima, H. (2006). Uptake pathways and subsequent intracellular trafficking in nonviral gene delivery. *Pharmacological Reviews*, Vol. 58, No. 1, (March 2006), pp. 32-45, ISSN 0031-6997
- Koltover, I.; Salditt, T.; Radler, J. O. & Safinya, C. R. (1998). An inverted hexagonal phase of cationic liposome-DNA complexes related to DNA release and delivery. *Science*, Vol. 281, No. 5373, (July 1998), pp. 78-81, ISSN 0036-8075.
- Kono, K.; Torikoshi, Y.; Mitsutomi, M.; Itoh, T.; Emi, N.; Yanagie, H. & Takagishi, T. (2001). Novel gene delivery systems: complexes of fusigenic polymer-modified liposomes and lipoplexes. *Gene Therapy*, Vol. 8, No. 1, (January 2001), pp. 5-12, ISSN 0969-7128.
- Koping-Hoggard, M.; Mel'nikova, Y. S.; Varum, K. M.; Lindman, B. & Artursson, P. (2003). Relationship between the physical shape and the efficiency of oligomeric chitosan as a gene delivery system in vitro and in vivo. *Journal of Gene Medicine*, Vol. 5, No. 2, (February 2003), pp. 130-141, ISSN 1099-498X.
- Krajcik, R.; Jung, A.; Hirsch, A.; Neuhuber, W. & Zolk, O. (2008). Functionalization of carbon nanotubes enables non-covalent binding and intracellular delivery of small interfering RNA for efficient knock-down of genes. *Biochemical and Biophysical Research Communications*, Vol. 369, No. 2, (May 2008), pp. 595-602, ISSN 0006-291X.
- Kucherlapati, R. & Skoultchi, A. I. (1984). Introduction of purified genes into mammalian-cells. *Crc Critical Reviews in Biochemistry*, Vol. 16, No. 4, (n.d. 1984), pp. 349-379, ISSN 0045-6411.
- Kumar, M. N. V. R.; Muzzarelli, R. A. A.; Muzzarelli, C.; Sashiwa, H. & Domb, A. J. (2004). Chitosan chemistry and pharmaceutical perspectives. *Chemical Reviews*, Vol. 104, No.12, (December 2004), pp. 6017-6084, ISSN 0009-2665.
- Kwon, B. & Kim, Y. (2008). Transient expression of an EP1-like gene encoded in Cotesia plutellae bracovirus suppresses the hemocyte population in the diamondback moth, *Plutella xylostella*. *Developmental and Comparative Immunology*, Vol. 32, No. 8, (n.d. 2008), pp. 932-942, ISSN 0145-305X.
- Lasic, D. D.; Strey, H.; Stuart, M. C. A.; Podgornik, R. & Frederik, P. M. (1997). The structure of DNA-liposome complexes. *JACS*, Vol. 119, No. 4, (January 1997), pp. 832-833, ISSN 0002-7863.
- Lavertu, M.; Methot, S.; Tran-Khanh, N. & Buschmann, M. D. (2006). High efficiency gene transfer using chitosan/DNA nanoparticles with specific combinations of molecular weight and degree of deacetylation. *Biomaterials*, Vol. 27, No. 27, (September 2006), pp. 4815-4824, ISSN 0142-9612.
- Lin, A. C. & Goh, M. C. (2002). Investigating the ultrastructure of fibrous long spacing collagen by parallel atomic force and transmission electron microscopy. *Proteins-Structure Function and Genetics*, Vol. 49, No. 3, (November 2002), pp. 378-384, ISSN 0887-3585.
- Lubyphelps, K.; Castle, P. E.; Taylor, D. L. & Lanni, F. (1987). Hindered diffusion of inert tracer particles in the cytoplasm of mouse 3T3 cells. *PNAS*, Vol. 84, No. 14, (July 1987), pp. 4910-4913, ISSN 0027-8424.



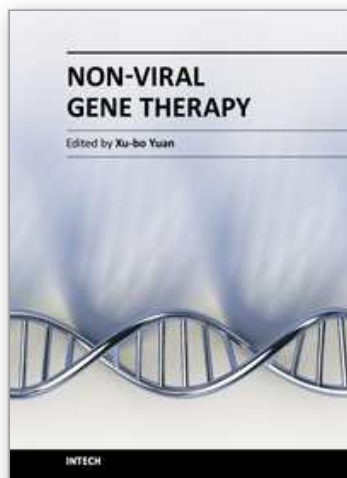
- Lynn, D. M. & Langer, R. (2000). Degradable poly( $\beta$ -amino esters): Synthesis, characterization, and self-assembly with plasmid DNA. *JACS*, Vol. 122, No. 44, (November 2000), pp. 10761-10768, ISSN 0002-7863.
- MacLaughlin, F. C.; Mumper, R. J.; Wang, J. J.; Tagliaferri, J. M.; Gill, I.; Hinchcliffe, M. & Rolland, A. P. (1998). Chitosan and depolymerized chitosan oligomers as condensing carriers for in vivo plasmid delivery. *Journal of Controlled Release*, Vol. 56, No. 1-3, (December 1998), pp. 259-272, ISSN 0168-3659.
- Mancheño-Corvo, P. & Martín-Duque, P. (2006). Viral gene therapy. *Clinical and Translational Oncology*, Vol. 8, No. 12, (n.d. 2006), pp. 858-867, ISSN 1699-048X.
- Manning, G. S. (1978). Molecular theory of polyelectrolyte solutions with applications to electrostatic properties of polynucleotides. *Quarterly Reviews of Biophysics*, Vol. 11, No. 2, (n.d. 1978), pp. 179-246, ISSN 0033-5835.
- Mao, H. Q.; Roy, K.; Troung-Le, V. L.; Janes, K. A.; Lin, K. Y.; Wang, Y.; August, J. T. & Leong, K. W. (2001). Chitosan-DNA nanoparticles as gene carriers: Synthesis, characterization and transfection efficiency. *Journal of Controlled Release*, Vol. 70, No. 3, (February 2001), pp. 399-421, ISSN 0168-3659.
- Marcelo, G.; Tarazona, M. P. & Saiz, E. (2005). Solution properties of poly (diallyldimethylammonium chloride) (PDDA). *Polymer*, Vol. 46, No. 8, (March 2005), pp. 2584-2594, ISSN 0032-3861.
- Matulis, D.; Rouzina, I. & Bloomfield, V. A. (2000). Thermodynamics of DNA binding and condensation: Isothermal titration calorimetry and electrostatic mechanism. *Journal of Molecular Biology*, Vol. 296, No. 4, (March 2000), pp. 1053-1063, ISSN 0022-2836.
- Maurstad, G.; Danielsen, S. & Stokke, B. T. (2007). The influence of charge density of chitosan in the compaction of the polyanions DNA and xanthan. *Biomacromolecules*, Vol. 8, No. 4, (April 2007), pp. 1124-1130, ISSN 1525-7797.
- Midoux, P.; Pichon, C.; Yaouanc, J. J. & Jaffres, P. A. (2009). Chemical vectors for gene delivery: A current review on polymers, peptides and lipids containing histidine or imidazole as nucleic acids carriers. *British Journal of Pharmacology*, Vol. 157, No. 2, (May 2009), pp. 166-178, ISSN 0007-1188.
- Miguel, M. G.; Pais, A. A. C. C.; Dias, R. S.; Leal, C.; Rosa, M. & Lindman, B. (2003). DNA-cationic amphiphile interactions. *Colloids and Surfaces A: Physicochemical and Engineering Aspects*, Vol. 228, No. 1-3, (November 2003), pp. 43-55, ISSN 0927-7757.
- Milev, S.; Bosshard, H. R. & Jelesarov, I. (2005). Enthalpic and entropic effects of salt and polyol osmolytes on site-specific protein-DNA association: The integrase Tn916-DNA complex. *Biochemistry*, Vol. 44, No. 1, (January 2005), pp. 285-293, ISSN 0006-2960.
- Mumper, R. J.; Wang, J. J.; Claspell, J. M. & Rolland, A. P. (1995). Novel polymeric condensing carriers for gene delivery. *Proceedings of the International Symposium on Controlled Release Bioactive Materials*, Vol. 22, pp. 178-179.
- Nguyen, D. N.; Green, J. J.; Chan, J. M.; Longer, R. & Anderson, D. G. (2009). Polymeric materials for gene delivery and DNA vaccination. *Advanced Materials*, Vol. 21, No. 8, (February 2009), pp. 847-867, ISSN 0935-9648.
- Nisha, C. K.; Manorama, S. V.; Ganguli, M.; Maiti, S. & Kizhakkedathu, J. N. (2004). Complexes of poly(ethylene glycol)-based cationic random copolymer and calf thymus DNA: A complete biophysical characterization. *Langmuir*, Vol. 20, No. 6, (March 2004), pp. 2386-2396, ISSN 0743-7463.

- Nuno-Donlucas, S. M.; Sanches-Diaz, J. C.; Rabelero, M.; Cortes-Ortega, J.; Luhrs-Olmos, C. C.; Fernandez-Escamilla, V. V.; Mendizabal, E. & Puig, J. E. (2004). Microstructured polyacrylamide hydrogels made with hydrophobic nanoparticles. *Journal of Colloid and Interface Science*, Vol. 270, No. 1, (February 2004), pp. 94-98, ISSN 0021-9797.
- O'Connor, T. P. & Crystal, R. G. (2006). Genetic medicines: Treatment strategies for hereditary disorders. *Nature Reviews Genetics*, Vol. 7, No. 4, (April 2006), pp. 261-276, ISSN 1471-0056.
- Ogris, M.; Steinlein, P.; Kurs, M.; Mechtler, K.; Kircheis, R. & Wagner, E. (1998). The size of DNA/transferrin-PEI complexes is an important factor for gene expression in cultured cells. *Gene Therapy*, Vol. 5, No. 10, (October 1998), pp. 1425-1433, ISSN 0969-7128.
- Orth, P.; Weimer, A.; Kaul, G.; Kohn, D.; Cucchiari, M. & Madry, H. (2008). Analysis of novel nonviral gene transfer systems for gene delivery to cells of the musculoskeletal system. *Molecular Biotechnology*, Vol. 38, No. 2, (February 2008), pp. 137-144, ISSN 1073-6085.
- Ota, K.; Matsumiya, T.; Sakuraba, H.; Imaizumi, T.; Yoshida, H.; Kawaguchi, S.; Fukuda, S. & Satoh, K. (2010). Interferon- $\alpha$ 2b induces p21<sup>cip1/waf1</sup> degradation and cell proliferation in HeLa cells. *Cell Cycle*, Vol. 9, No. 1, (January 2010), pp. 131-139, ISSN 1538-4101.
- Prevette, L. E.; Kodger, T. E.; Reineke, T. M. & Lynch, M. L. (2007). Deciphering the role of hydrogen bonding in enhancing pDNA-Polycation interactions. *Langmuir*, Vol. 23, No. 19, (September 2007), pp. 9773-9784, ISSN 0743-7463.
- Privalov, P. L.; Dragan, A. I.; Crane-Robinson, C.; Breslauer, K. J.; Remeta, D. P. & Minetti, C. (2007). What drives proteins into the major or minor grooves of DNA? *Journal of Molecular Biology*, Vol. 365, No. 1, (January 2007), pp. 1-9, ISSN 0022-2836.
- Radler, J. O.; Koltover, I.; Salditt, T. & Safinya, C. R. (1997). Structure of DNA-cationic liposome complexes: DNA intercalation in multilamellar membranes in distinct interhelical packing regimes. *Science*, Vol. 275, No. 5301, (February 1997), pp. 810-814, ISSN 0036-8075.
- Rau, D. C. & Parsegian, V. A. (1992). Direct measurement of the intermolecular forces between counterion-condensed DNA double helices: Evidence for long-range attractive hydration forces. *Biophysical Journal*, Vol. 61, No. 1, (January 1992), pp. 246-259, ISSN 0006-3495.
- Rejman, J.; Oberle, V.; Zuhorn, I. S. & Hoekstra, D. (2004). Size-dependent internalization of particles via the pathways of clathrin- and caveolae-mediated endocytosis. *Biochemical Journal*, Vol. 377 (January 2004), pp. 159-169, ISSN 0264-6021.
- Rodriguez-Pulido, A.; Aicart, E.; Llorca, O. & Junquera, E. (2008). Compaction process of calf thymus DNA by mixed cationic-zwitterionic liposomes: A physicochemical study. *J. Phys. Chem. B*, Vol. 112, No. 7, (February 2008), pp. 2187-2197, ISSN 1520-6106.
- Ruozi, B.; Tosi, G.; Leo, E. & Vandelli, M. A. (2007). Application of atomic force microscopy to characterize liposomes as drug and gene carriers. *Talanta*, Vol. 73, No. 1, (August 2007), pp. 12-22, ISSN 0039-9140.
- Sahay, G.; Alakhova, D. Y. & Kabanov, A. V. (2010). Endocytosis of nanomedicines. *Journal of Controlled Release*, Vol. 145, No. 3, (August 2010), pp. 182-195, ISSN 0168-3659.

- Salditt, T.; Koltover, I.; Radler, J. O. & Safinya, C. R. (1997). Two-dimensional smectic ordering of linear DNA chains in self-assembled DNA-cationic liposome mixtures. *PRL*, Vol. 79, No. 13, (September 1997), pp. 2582-2585, ISSN 0031-9007.
- Sarraguca, J. M. G. & Pais, A. A. C. C. (2006). Polyelectrolytes in solutions with multivalent salt. Effects of flexibility and contour length. *Phys. Chem. Chem. Phys.*, Vol. 8, No. 36, (n.d. 2006), pp. 4233-4241, ISSN 1463-9076.
- Schaffer, D. V.; Fidelman, N. A.; Dan, N. & Lauffenburger, D. A. (2000). Vector unpacking as a potential barrier for receptor-mediated polyplex gene delivery. *Biotechnology and Bioengineering*, Vol. 67, No. 5, (March 2000), pp. 598-606, ISSN 0006-3592.
- Silverstein, K. A. T.; Haymet, A. D. J. & Dill, K. A. (2000). The strength of hydrogen bonds in liquid water and around nonpolar solutes. *JACS*, Vol. 122, No. 33, (August 2000), pp. 8037-8041, ISSN 0002-7863.
- Simberg, D.; Weisman, S.; Talmon, Y. & Barenholz, Y. (2004). DOTAP (and other cationic lipids): Chemistry, biophysics, and transfection. *Critical Reviews in Therapeutic Drug Carrier Systems*, Vol. 21, No. 4, (n.d. 2004), pp. 257-317, ISSN 0743-4863.
- Simoes, S.; Slepishkin, V.; Gaspar, R.; de Lima, M. C. P. & Duzgunes, N. (1998). Gene delivery by negatively charged ternary complexes of DNA, cationic liposomes and transferrin or fusigenic peptides. *Gene Therapy*, Vol. 5, No. 7, (July 1998), pp. 955-964, ISSN 0969-7128.
- Spinosa, M. R.; Progida, C.; De Luca, A.; Colucci, A. M. R.; Alifano, P. & Bucci, C. (2008). Functional characterization of Rab7 mutant proteins associated with Charcot-Marie-Tooth type 2B disease. *Journal of Neuroscience*, Vol. 28, No. 7, (February 2008), pp. 1640-1648, ISSN 0270-6474.
- Srinivasachari, S.; Liu, Y. M.; Prevette, L. E. & Reineke, T. M. (2007). Effects of trehalose click polymer length on pDNA complex stability and delivery efficacy. *Biomaterials*, Vol. 28, No. 18, (June 2007), pp. 2885-2898, ISSN 0142-9612.
- Sternberg, B.; Sorgi, F. L. & Huang, L. (1994). New structures in complex-formation between DNA and cationic liposomes visualized by freeze-fracture electron-microscopy. *Febs Letters*, Vol. 356, No. 2-3, (December 1994), pp. 361-366, ISSN 0014-5793.
- Strand, S. P.; Lelu, S.; Reitan, N. K.; de Lange Davies, C.; Artursson, P. & Varum, K. M. (2010). Molecular design of chitosan gene delivery systems with an optimized balance between polyplex stability and polyplex unpacking. *Biomaterials*, Vol. 31, No. 5, (February 2010), pp. 975-87, ISSN 1878-5905.
- Strey, H. H.; Podgornik, R.; Rau, D. C. & Parsegian, V. A. (1998). DNA-DNA interactions. *Current Opinion in Structural Biology*, Vol. 8, No. 3, (June 1998), pp. 309-313, ISSN 0959-440X.
- Tang, M. X. & Szoka, F. C. (1997). The influence of polymer structure on the interactions of cationic polymers with DNA and morphology of the resulting complexes. *Gene Therapy*, Vol. 4, No. 8, (August 1997), pp. 823-832, ISSN 0969-7128.
- Thakor, D. K.; Teng, Y. D. & Tabata, Y. (2009). Neuronal gene delivery by negatively charged pullulan-spermine/DNA anioplexes. *Biomaterials*, Vol. 30, No. 9, (March 2009), pp. 1815-1826, ISSN 0142-9612.
- Thomas, M. & Klibanov, A. M. (2003). Non-viral gene therapy: polycation-mediated DNA delivery. *Applied Microbiology and Biotechnology*, Vol. 62, No. 1, (July 2003), pp. 27-34, ISSN 0175-7598.

- Toncheva, V.; Wolfert, M. A.; Dash, P. R.; Oupicky, D.; Ulbrich, K.; Seymour, L. W. & Schacht, E. H. (1998). Novel vectors for gene delivery formed by self-assembly of DNA with poly(L-lysine) grafted with hydrophilic polymers. *Biochimica Et Biophysica Acta: General Subjects*, Vol. 1380, No. 3, (May 1998), pp. 354-368, ISSN 0304-4165.
- Tros de Ilarduya, C.; Sun, Y. & Düzgünes, N. (2010). Gene delivery by lipoplexes and polyplexes. *European Journal of Pharmaceutical Sciences*, Vol. 40, No. 3, (June 2010), pp. 159-170, ISSN 0928-0987.
- Trzcinski, S.; Varum, K. M.; Staszewska, D. U.; Smidsrod, O. & Bohdanecky, M. (2002). Comparative studies on molecular chain parameters of chitosans and poly(diallyldimethylammonium chloride): The stiffness B-parameter and the temperature coefficient of intrinsic viscosity. *Carbohydrate Polymers*, Vol. 48, No. 2, (May 2002), pp. 171-178, ISSN 0144-8617.
- Verma, I. M. & Somia, N. (1997). Gene therapy: Promises, problems and prospects. *Nature*, Vol. 389, No. 6648, (September 1997), pp. 239-242, ISSN 0028-0836.
- Wagner, E.; Cotten, M.; Foisner, R. & Birnstiel, M. L. (1991). Transferrin polycation DNA complexes: The effect of polycations on the structure of the complex and DNA delivery to cells. *PNAS*, Vol. 88, No. 10, (May 1991), pp. 4255-4259, ISSN 0027-8424.
- Wandrey, C.; Hernandez-Barajas, J. & Hunkeler, D. (1999). Diallyldimethylammonium chloride and its polymers. *Radical Polymerisation Polyelectrolytes*, Vol. 145, (n.d. 1999), pp. 123-182, ISSN 0065-3195.
- Wang, C. Z.; Li, X. F.; Wettig, S. D.; Badea, I.; Foldvari, M. & Verrall, R. E. (2007). Investigation of complexes formed by interaction of cationic gemini surfactants with deoxyribonucleic acid. *Phys. Chem. Chem. Phys.*, Vol. 9, No. 13, (n.d. 2007), pp. 1616-1628, ISSN 1463-9076.
- Wilson, R. W. & Bloomfield, V. A. (1979). Counterion-induced condensation of deoxyribonucleic acid. A light-scattering study. *Biochemistry*, Vol. 18, No. 11, (May 1979), pp. 2192-2196, ISSN 0006-2960.
- Wu, G. Y. & Wu, C. H. (1987). Receptor-mediated in vitro gene transformation by a soluble DNA carrier system. *JBC*, Vol. 262, No. 10, (April 1987), pp. 4429-4432.
- Ziady, A. G.; Ferkol, T.; Dawson, D. V.; Perlmutter, D. H. & Davis, P. B. (1999). Chain length of the polylysine in receptor-targeted gene transfer complexes affects duration of reporter gene expression both in vitro and in vivo. *JBC*, Vol. 274, No. 8, (February 1999), pp. 4908-4916, ISSN 0021-9258.





### **Non-Viral Gene Therapy**

Edited by Prof. Xubo Yuan

ISBN 978-953-307-538-9

Hard cover, 696 pages

**Publisher** InTech

**Published online** 07, November, 2011

**Published in print edition** November, 2011

This book focuses on recent advancement of gene delivery systems research. With the multidisciplinary contribution in gene delivery, the book covers several aspects in the gene therapy development: various gene delivery systems, methods to enhance delivery, materials with modification and multifunction for the tumor or tissue targeting. This book will help molecular biologists gain a basic knowledge of gene delivery vehicles, while drug delivery scientist will better understand DNA, molecular biology, and DNA manipulation.

### **How to reference**

In order to correctly reference this scholarly work, feel free to copy and paste the following:

Manuel Alatorre-Meda, Eustolia Rodríguez-Velázquez and Julio R. Rodríguez (2011). Polycation-Mediated Gene Delivery: The Physicochemical Aspects Governing the Process, Non-Viral Gene Therapy, Prof. Xubo Yuan (Ed.), ISBN: 978-953-307-538-9, InTech, Available from: <http://www.intechopen.com/books/non-viral-gene-therapy/polycation-mediated-gene-delivery-the-physicochemical-aspects-governing-the-process>

**INTECH**  
open science | open minds

### **InTech Europe**

University Campus STeP Ri  
Slavka Krautzeka 83/A  
51000 Rijeka, Croatia  
Phone: +385 (51) 770 447  
Fax: +385 (51) 686 166  
[www.intechopen.com](http://www.intechopen.com)

### **InTech China**

Unit 405, Office Block, Hotel Equatorial Shanghai  
No.65, Yan An Road (West), Shanghai, 200040, China  
中国上海市延安西路65号上海国际贵都大饭店办公楼405单元  
Phone: +86-21-62489820  
Fax: +86-21-62489821



© 2011 The Author(s). Licensee IntechOpen. This is an open access article distributed under the terms of the [Creative Commons Attribution 3.0 License](https://creativecommons.org/licenses/by/3.0/), which permits unrestricted use, distribution, and reproduction in any medium, provided the original work is properly cited.

IntechOpen

IntechOpen